**UNIVERSITY OF CALGARY**

# Alterations in Current Density and Transmural Regional Heterogeneity of Cardiac Repolarization $K^+$ Currents in Left Ventricular Hypertrophy

by

Radzfel Geonzon

A THESIS

SUBMITTED TO THE FACULTY OF GRADUATE STUDIES

IN PARTIAL FULFILLMENT OF THE REQUIREMENTS FOR THE

DEGREE OF MASTER OF SCIENCE

DEPARTMENT OF CARDIOVASCULAR/RESPIRATORY SCIENCES

CALGARY, ALBERTA

MARCH, 2000

## Abstract

Cardiac left ventricular hypertrophy (LVH) is initially an adaptive response of the heart to haemodynamic overload. However, chronic hypertrophy becomes maladaptive and contributes to the pathophysiology leading to arrhythmia and congestive heart failure. In most situations associated with LVH, there is a prolongation of action potential duration (APD) and an increase in ventricular dispersion of repolarization. Previous studies have attributed the prolongation of APD and the subsequent alterations in dispersion of repolarization to various ionic currents that have been modulated in LVH. We hypothesized that the cardiac $K^+$ channel response to hypertrophy would be spatially heterogeneous and that the effects of acute administration of $\alpha_1$-adrenergic agonists on the repolarizating $K^+$ currents in LVH conditions would differ in control versus hypertrophied animals. Male New Zealand white rabbits were randomly assigned to two groups, cardiac hypertrophy and age matched controls. Abdominal aortic banding resulted in statistically significant increases in blood pressure from 104/77 to 159/110 mmHg, increases in ventricular wet weight/body weight ratio from 3.3±0.4 to 3.6±0.4 g/kg, and increases in ventricular cell capacitance from 140±53pF (endocardium) and 132±3pF (epicardium) to 173±63pF and 161±29pF respectively. Cardiac hypertrophy also resulted in a decrease of $I_{to}$ current density at +40mV from 11±4 to 9±4pA/pF in endocardium and from 13±5 to 8±5pA/pF in epicardium ($p<0.05$). The magnitude of $I_{to}$ reduction was greater in epicardium (35±8%) than in endocardium (18±6%;$p<0.05$). In contrast, $I_{K1}$ current density was significantly decreased in endocardium, but not in epicardium. The

tail current density of $I_{Kr}$ was greater in endocardium than epicardium and this difference was exaggerated by LVH. This difference in transmural $I_{Kr}$ tail current density suggested the presence of spatial regional heterogeneity with rabbit $I_{Kr}$. In addition, $I_{to}$ response to 100μM methoxamine (given *in vitro*) was significantly less in endocardial myocytes from hypertrophied (26±7%block) compared to control (49±5%block) rabbits. Conclusion: LVH alters the current density of $I_{to}$ and $I_{K1}$ in a spatially heterogeneous manner and that the response to *in vitro* methoxamine was less in LVH than in control rabbit hearts. In addition, transmural rabbit $I_{Kr}$ tail current density is spatially heterogeneous and this regional dispersion is exaggerated in LVH. These observations suggest a mechanism for the prolongation of APD and the increase in dispersion of repolarization often seen in LVH.

## Table of Contents

## List of Tables

## List of Figures

# Introduction : Chapter 1

In mammalian physiology, there are many examples where physiologic processes have both an adaptive and maladaptive response to underlining physiological environmental stresses. One example that is of great interest is the involvement of the $\alpha_1$-adrenergic receptor in the development of cardiac hypertrophy. In normal cardiac growth and development, previous studies have found that the $\alpha_1$-adrenergic receptor contributes to developmental myocardial hypertrophy seen in neonatal cardiac myocytes in various mammalian species (LaMorte *et al.,* 1994, Simpson *et al.,* 1991, Li *et al.,* 1997). This is an example of an adaptive response to changes in the physiological environment. Ironically, the $\alpha_1$-adrenergic receptor has also been found to strongly contribute to the development of pathological cardiac hypertrophy, which is a maladaptive response. The involvement of the $\alpha_1$-adrenergic receptor in pathological cardiac hypertrophy is a vast and complex physiological process that has been a very important area of research in the medical field. This project examines the modulation of cardiac repolarizating $K^+$ currents in left ventricular cardiac hypertrophy (LVH) as well as the effects of acute administration of the selective $\alpha_1$-adrenergic agonist (Methoxamine) on these $K^+$ currents in LVH.

## 1.1 The α-Adrenergic Receptor

FUNCTION

The α-adrenergic receptors are receptors that bind adrenergic hormones like norepinephrine. In normal acute physiologic conditions, α-adrenergic receptors promote vascular vasoconstriction, by stimulating smooth muscle contraction. In the heart, activation of myocardial $\alpha_1$-adrenergic receptors have been shown to increase the force of contraction and have positive inotropic effects (Endoh *et al.,* 1988, Hescheler *et al.,* 1988). In normal chronic physiologic conditions, α-adrenergic receptors are partly involved in increasing protein synthesis and activity of gene promoters, mitogen activated protein kinases (MAPK) and other transcription factors that are involved in normal (and possibly abnormal) myocardial growth and gene expression (Bogoyevitch *et al.,* 1996, Simpson *et al.,* 1991).

SUBTYPES

α-Adrenergic receptors can be divided into two main subtypes, $\alpha_1$ and $\alpha_2$. In addition, the $\alpha_1$ and $\alpha_2$ subtypes can be further subdivided into homologous family members ($\alpha_1$a, $\alpha_1$b, $\alpha_1$c, $\alpha_1$d and $\alpha_2$a, $\alpha_2$b, $\alpha_2$c) (Rokosh *et al.,* 1996, Rohrer *et al.,* 1998). At present, the evidence suggests that the predominant α-adrenergic receptor subtype in cardiac myocytes is the $\alpha_1$-subtype. This has been shown through the use of selective $\alpha_1$-agonists like methoxamine and phenylephrine and selective $\alpha_1$-

antagonists like prazosin and phentolamine (Fedida *et al.,* 1993). In a single myocyte, $\alpha_1$ -adrenergic stimulation has lead to a variety of cellular responses, including changes in contractility and/or excitability, metabolic alterations and with time, changes in gene expression/cellular hypertrophy (Fedida *et al.,* 1993). It is the $\alpha_1$ -adrenergic receptor, which has been shown to have a prominent role in the development of LVH (Fedida *et al.,* 1993, Meszaros *et al.,* 1996, Milano *et al.,* 1994). Thus, this project will focus only on the effects of the $\alpha_1$ -adrenergic receptor and its involvement in LVH.

Since the focus of this project is on cardiac electrophysiology in LVH, a short overview of the electrophysiological parameters to be studied is provided below.

## 1.2 Cardiac Action Potential

In normal myocardium, cardiac electrical signals are transmitted by action potentials firing at regular intervals. Action potentials are rapid all-or-none changes in the membrane potential, which are initiated by spontaneous depolarizations of the membrane potential. The action potential is a sign of changes in the polarization of the cell membrane; a redistribution of electrical charge brought about by the translocation of ions (Milnor, 1990). In a normal cardiac myocyte, the resting membrane potential is about –80mV. The negativity of the resting membrane potential is largely due to the permeability of the membrane to $K^+$ ions. This permeability to $K^+$ results in a resting membrane potential that is near the equilibrium

potential of $K^+$ (-90 to -100mV). A minor contributor to the cardiac resting membrane potential is the action of membrane bound cardiac $Na^+/K^+$ pumps that pump more positive charges outside of the cell than inside (3 $Na^+$ outside to 2 $K^+$ inside) (Guyton, 1991). An action potential occurs when there is a sudden and rapid change in membrane potential to more depolarized levels that are past the excitation threshold of the $Na^+$ channel. This depolarization of the membrane potential results in a rapid and complete depolarization that lasts for a few hundred milliseconds (in heart) and then returns back to the initial state of the resting membrane potential. According to Milnor, the condition that initiates an action potential is not, however, the membrane voltage per se but a change from net outward to inward current (Milnor, 1990).

## PHASES OF A CARDIAC ACTION POTENTIAL

The cardiac action potential is comprised of 5 successive phases. The action potential begins with phase 0. This phase is described as a very rapid depolarization that is so large that it reverses the membrane polarity. This fast upstroke is predominantly due to activation of the inward sodium current, $I_{Na}$. Once the action potential reaches its most positive peak, the $Na^+$ channels inactivate and the potential repolarizes (phase 1). This phase 1 repolarization is largely due to the activation of depolarization-activated outward $K^+$ currents. Also in phase 1, the L-type $Ca^{2+}$ current ($I_{Ca}$) is activated. The resulting action potential plateau (phase 2) that is characteristic of cardiac action potentials is the result of a balance between the depolarization-activated outward $K^+$ currents and the inward L-type $Ca^{2+}$ current.

During phase 3 of the action potential, $I_{Ca}$ is inactivated and thus the predominant currents left are outward $K^+$ currents that rapidly repolarize the membrane back to its previous polarized state and end the action potential. Phase 4 is the period between action potentials. The membrane potential during this period is determined by activated $Na^+/K^+$ pumps and the inwardly rectifying $K^+$ current.

## 1.3 Dispersion of Ventricular Repolarization

Dispersion of ventricular repolarization can be described as a gradient of action potential duration (APD) in the ventricles that result in heterogeneous ventricular repolarization. In normal hearts, repolarization of the ventricles starts at the epicardium and moves transmurally to the endocardium (Antzelevitch *et al.*, 1998, McIntosh *et al.*, 1998). This gradient of repolarization can be explained by work done by Casis *et al.*, 1998 and Fedida *et al.*, 1991. In both rabbit and rat ventricles, the APD was found to be shorter in the epicardium and longer in the endocardium (Casis *et al.*, 1998, Fedida *et al.*, 1991). A shorter APD in the epicardium reflects a shorter repolarization time seen in the epicardium. Their observations would also explain the longer repolarization time seen in the endocardium as well. In addition, dispersion of ventricular repolarization can be measured along the apicobasal and anteroposterior axes as well (Antzelevitch *et al.*, 1998, Gillis *et al.*, 1998). However, according to Antzelevitch *et al.*, transmural heterogeneities in repolarization time are more abrupt than those recorded along the surfaces of the heart. These transmural heterogeneities may represent a more

suitable substrate for the development of arrhythmias and their quantitation may provide a valuable tool for evaluation of arrhythmia risk (Antzelevitch *et al.,* 1998).

Since there are so many currents involved in the generation and maintenance of a cardiac action potential, not all currents can be examined in this project. Therefore, this project will focus on the repolarizating $K^+$ currents involved in the cardiac action potential and their LVH-induced modulations. But first, what is LVH?

## 1.4 Cardiac Left Ventricular Hypertrophy

Cardiac left ventricular hypertrophy (LVH) is an adaptive response of the heart to haemodynamic overload (Tamai *et al.,* 1989). Disease states like hypertension and valvular heart disease expose the myocardium to chronic pressure or volume overload (Schunkert *et al.,* 1995, Tamai *et al.,* 1989). According to Schunkert et al., cardiac myocytes are terminally differentiated cells without the ability to divide and thus, cellular hypertrophy is the dominant mechanism to normalize the persisting elevation of systolic wall stress under these conditions (Schunkert *et al.,* 1995). In the later stages of chronic pressure overload, the heart's ability to compensate for the rapidly developing abnormal conditions would diminish. The final result would be cell loss, progressive fibrosis, impairment of diastolic and systolic function, as well as the development of other characteristics of hypertensive heart disease and congestive heart failure (Schunkert *et al.,* 1995). Myocardial stress induced by pressure overload results in alterations in the pattern of myocardial gene expression, substantial remodeling of the heart's geometry, and regression to a fetal pattern of cellular biology, which lead to the development of LVH (Calderone *et al.*, 1995, Schunkert *et al.,* 1995). For example, previous studies have shown an increase in mRNA levels for the fetal genes β-myosin heavy chain and skeletal α-actin in pressure overload-induced LVH (Calderone *et al.*, 1995). Moreover, LVH has been associated with an increased risk of cardiac arrhythmias in both patients and in experimental animals (McIntosh *et al.*, 1998).

## ACTION POTENTIAL PROLONGATION

There is consistent evidence that pressure overload-induced cardiac hypertrophy is accompanied by a prolongation of the cardiac action potential duration (APD) (Gillis *et al.,* 1998, McIntosh *et al.,* 1998, Nabauer *et al.,* 1998). This prolongation of APD can in part contribute to the proarrhythmic conditions in LVH by lengthening the $Ca^{2+}$ plateau of the cardiac action potential and increasing the risk of after-depolarizations (EADs) due to $Ca^{2+}$ overload. In the paper by McIntosh *et al.,* the authors showed that APD was prolonged in rabbits that developed perinephritis-induced LVH. However, the change seen was regionally dependent. They stated that in controls, endocardial APD was longer than epicardial APD. In LVH, both endocardial and epicardial APD were prolonged, but it was shown that epicardial APD was significantly longer than endocardial APD. This regional heterogeneity of prolongation of ventricular APD reflects the electrophysiological phenomenon described earlier known as dispersion of ventricular repolarization.

## INCREASE IN DISPERSION OF VENTRICULAR REPOLARIZATION

Closely related to the prolongation of APD in LVH is the increase of dispersion of ventricular repolarization in LVH. According to Gillis *et al.* in rabbit, dispersion of ventricular repolarization is shown to increase in the settings of LVH, congestive heart failure, post myocardial infarction, torsades de pointes ventricular

tachycardia and congenital long QT syndrome (Gillis *et al.,* 1998). Also, increased dispersion of ventricular repolarization can lead to a predisposition to arrhythmia development as well as sudden cardiac death. The level of dispersion of repolarization can be measured by the difference between the maximal and minimal APD (Gillis *et al.,* 1998) measured from different areas of the heart. According to McIntosh *et al.,* a possible consequence of these differences in APD would be an alteration of the normal pattern of ventricular repolarization. This alteration could explain the inversion of the ECG T-wave, which has been associated with the occurrence of hypertrophy in patients and could provide the basis for the development of abnormal cardiac rhythm (McIntosh *et al.,* 1998, Shipsey *et al.,* 1997, Shimizu *et al.,* 1999).

## 1.5 Changes in Repolarizing $K^+$ Currents in LVH

McIntosh, as well as others have attributed the prolongation of APD and the subsequent alterations in dispersion of ventricular repolarization to various ionic currents that have been modulated in LVH (Antzelevitch *et al.*, 1998, Gillis *et al.*, 1998, McIntosh *et al.*, 1998, Meszaros *et al.*, 1996, Potreau *et al.*, 1995, Tomita *et al.*, 1994).

### THE TRANSIENT OUTWARD CURRENT ($I_{to}$)

$I_{to}$ is thought to consist of at least two components: a voltage-dependent, $Ca^{2+}$-independent, and 4-aminopyridine (4-AP) sensitive component and a $Ca^{2+}$-dependent, 4-AP-insensitive component (Giles *et al.*, 1985, Siegelbaum and Tsien, 1980). According to Giles *et al.*, the major transient outward current in rabbit heart is of the $Ca^{2+}$-independent type (Giles *et al.*, 1988, Braun *et al.*, 1990). Thus, the focus of this study will be on the $Ca^{2+}$-independent, 4-AP sensitive component of $I_{to}$. $I_{to}$ is involved during phase 1 repolarization of the cardiac action potential. It is responsible for the repolarization "notch" seen right after the $I_{Na}$ upstroke.

### LVH EFFECTS ON THE TRANSIENT OUTWARD $K^+$ CURRENT

In the literature, $I_{to}$ current density has consistently been shown to be significantly depressed in hypertrophied cardiac myocytes, which would have a significant prolonging effect on the APD (Meszaros *et al.*, 1996, Potreau *et al.*, 1995, Tomita *et*

*al.,* 1994). Experimental cardiac hypertrophies induced in rats (aortic banding and catecholamine-treated) have shown a decrease in $I_{to}$ density without significant alterations in the kinetic properties (McIntosh *et al.,* 1998, Meszaros *et al.,* 1996, Tomita *et al.,* 1994). Steady-state inactivation, the inactivation time course, and the time course of recovery from inactivation were very similar in normal and hypertrophied cells (McIntosh *et al.,* 1998, Meszaros *et al.,* 1996, Tomita *et al.,* 1994). My own studies with Gillis *et al.,* showed that $I_{to}$ had reduced current densities in rabbit LVH cardiac myocytes as well (Gillis *et al.,* 1998, McIntosh *et al.,* 1998). In contrast, depressed $I_{to}$ in single hypertrophied cardiomyocytes isolated from the right ventricle of a ferret heart displayed a decrease in current density, as well as alterations in kinetics (Potreau *et al.,* 1995). In addition, previous literature have shown that there was a differential distribution of functional $I_{to}$ channel density (Giles *et al.,* 1991, Liu *et al.,* 1993, McIntosh *et al.,* 1998). This regional heterogeneity of $I_{to}$ can explain the regional differences in APD seen between endocardial and epicardial myocytes of normal and hypertrophied hearts as well as LVH alterations in dispersion of ventricular repolarization.

## THE INWARDLY RECTIFYING $K^+$ CURRENT ($I_{K1}$)

Cardiac $I_{K1}$ is $K^+$ selective and is sensitive to barium (Sakmann *et al.,* 1984, DiFrancesco *et al.,* 1984). $I_{K1}$ passes $K^+$ preferentially in the inward direction at membrane potentials negative to the equilibrium potential for $K^+$ ($E_K$), but shows a profoundly reduced conductance in the outward direction at membrane potentials positive to $E_K$ (Hille B, 1992). This property is referred to as inward rectification. $I_{K1}$ is

dominantly involved in maintaining the resting membrane potential of the cardiac myocyte. It also contributes to late phase 3 and phase 4 repolarization of the cardiac action potential.

## LVH EFFECTS ON THE INWARDLY RECTIFYING $K^+$ CURRENT

According to the review done by Nabauer *et al.,* there were conflicting views on the effect of LVH on $I_{K1}$. It was reported that $I_{K1}$ was increased in mildly hypertrophied feline right ventricular myocytes after pulmonary artery banding. However in rat with spontaneous hypertension and guinea pig with mild hypertrophy due to abdominal aortic constriction, no changes in $I_{K1}$ current density were observed (Nabauer *et al.,* 1998). Interestingly, McIntosh *et al.,* showed a significant decrease in $I_{K1}$ in both the outward and inward portion of the current in perinephritis-induced LVH in rabbit. Also, it was found that the reduction in $I_{K1}$ in their model was similar in both the epicardium and endocardium (McIntosh *et al.,* 1998). In addition, Casis *et al.,* found no significant changes in $I_{K1}$ density between the right ventricle, left ventricular subepicardium from the heart apex and left ventricular subendocardium from the heart base in normal rats (Casis *et al.,* 1998). This suggests that $I_{K1}$ is relatively regionally homogeneous.

## THE DELAYED RECTIFYER $K^+$ CURRENT ($I_K$)

$I_K$ is comprised of two components: a rapid activating and dofetilide (Class III antiarrhythmic drug)-sensitive current ($I_{Kr}$), which is inwardly rectifying and a slow

activating and dofetilide-resistant current ($I_{Ks}$) which is outwardly rectifying. $I_K$ is activated during phase 3 of the cardiac action potential. In rabbit, $I_K$ density is larger in atrium than in ventricle, but is much smaller than $I_{to}$ in both cell types (Giles *et al.*, 1988). Due to its small size, $I_K$ contributes only a small repolarizing influence on the action potential. Based on their observations, Giles *et al.* concluded that the action potential configuration in rabbit ventricular myocytes were mainly due to $I_{to}$ and $I_{K1}$ (Giles *et al.*, 1988).

## LVH EFFECTS ON THE DELAYED RECTIFYER $K^+$ CURRENT

Nabauer *et al.* reported that $I_K$ was reduced in hypertrophied feline right and left ventricular myocytes after pulmonary artery banding and abdominal aortic constriction respectively (Nabauer *et al.*, 1998). However in guinea pig with mild hypertrophy due to abdominal aortic constriction, no changes in $I_K$ current density were observed (Nabauer *et al.*, 1998). In addition, Casis *et al.*, found no significant change in $I_K$ current density between the right ventricle, left ventricular subepicardium from the heart apex and left ventricular subendocardium from the heart base in normal rats (Casis *et al.*, 1998). This suggested that $I_K$, in their animal model, was regionally homogeneous. As an interesting note, Casis *et al.*, based their observations on the activating outward current only. No $I_K$ tails were recorded. Moreover, the regional distributions of $I_K$ in the conditions of LVH have not yet been examined. Possible reasons for this could be a lack of a good animal model to study $I_K$ regional differences. It is known that guinea pigs have a relatively large $I_K$, however, the size of the heart in guinea pigs might prove too difficult to conduct

proper and accurate measurements of $I_K$ regional distribution. In addition, rabbit hearts are large enough for accurate measurements of ion current regional distribution. But as was stated earlier, $I_K$ was not among the dominant $K^+$ currents in rabbit heart and its contribution to rabbit action potential repolarization was considered small. Thus, most researchers examining rabbit action potentials and the underlining repolarization $K^+$ currents have only studied $I_{to}$ and $I_{K1}$ due to their dominance in the configuration of the rabbit action potential.

## 1.6 LVH and the $\alpha_1$ -Adrenergic Receptor

### $\alpha_1$-ADRENERGIC TRANSMEMBRANE SIGNALING MECHANISMS

The coupling of the $\alpha_1$-adrenergic receptors to the final cell response involves a complex chain of intracellular reactions. Through a G-protein mediated pathway, $\alpha_1$-adrenergic stimulation results in the increase of intracellular $Ca^{2+}$ stores and the breakdown of phosphoinositides to inositol-triphosphate and diacyglycerol (Milnor, 1990). Inositol-triphosphate triggers the release of $Ca^{2+}$ from intracellular stores and may also affect $Ca^{2+}$ entry through the membrane (Milnor, 1990). An increase in intracellular $Ca^{2+}$ activates other second messengers like calmodulin, which can activate kinases like CAMKII that can phosphorylate membrane proteins like ionic channels (Fedida *et al.,* 1993, Guo *et al.,* 1998). Diacyglycerol has been associated with the protein kinase C (PKC) pathway. It activates PKC, which is capable of phosphorylating myosin light chains and other proteins (membrane-bound and cytosolic) (Fedida *et al.,* 1993, Milnor, 1990). In addition, distribution of sympathetic innervation (adrenergic) is generally greater in epicardium than endocardium in many species (Crick *et al.,* 1999, Slavikova *et al.,* 1993). Thus, effects of cardiac adrenergic stimulation may be transmurally heterogeneous.

## CHRONIC EFFECTS

In the manuscript by Milano *et al.,* transgenic mice were generated by using the alpha-myosin heavy chain promoter coupled to the coding sequence of a constitutively active mutant $\alpha_{1B}$-adrenergic receptor (Milano *et al.,* 1994). In these mice, a phenotype consistent with cardiac hypertrophy developed in the adults with increased heart/body weight ratios, increased myocyte cross-sectional areas, and increased ventricular atrial natriuretic factor mRNA levels relative to nontransgenic controls (Milano *et al.,* 1994). In addition, the surface density of $\alpha_1$-adrenergic receptors has been shown to be increased in many models of cardiac hypertrophy (Hayashi *et al.,* 1995, Imai *et al.,* 1995, Tamai *et al.,* 1989). The increase in surface receptor density has been shown to increase the sensitivity of the myocardium to $\alpha_1$-adrenergic stimulation (Fedida *et al.,* 1993, Wilber *et al.,* 1987) This hypersensitivity may lead to arrhythmias especially under ischemic conditions (Corr *et al.*, 1981, Corr *et al.,* 1989, Dillon *et al.,* 1988, Fedida *et al.,* 1993.)

## ACUTE EFFECTS

Acute stimulation of the $\alpha_1$-adrenergic receptor by selective agonists (i.e., phenylephrine and methoxamine) has been shown to depress $I_{to}$ and $I_{K1}$ and prolong the APD (Braun *et al.,* 1990, Braun *et al.,* 1992, Fedida *et al.,* 1993). Acute studies with guinea pig ventricular myocytes showed that $\alpha_1$-adrenergic stimulation could upregulate $I_K$ through a PKC-dependent pathway (Tohse *et al.,* 1992). In rabbit ventricular myocytes, acute studies have demonstrated that $\alpha_1$-adrenergic

stimulation resulted in the downregulation of $I_{K1}$ and $I_{to}$ through a signal transduction pathway that was apparently PKC-independent (Braun *et al.,* 1990, Fedida *et al.,* 1991).

## THE INSIGHT

Based on the above observations, the LVH-induced increase in $\alpha_1$-adrenergic receptor density might be a contributing factor in the chronic modulation of cardiac repolarization $K^+$ currents and subsequent APD prolongation and dispersion of ventricular repolarization seen in LVH. Moreover, the effects of acute administration of $\alpha_1$-adrenergic agonists on the repolarization $K^+$ currents in LVH conditions have not yet been examined.

## Hypotheses : Chapter 2

1. LVH exaggerates the regional heterogeneity of repolarizating $K^+$ currents in rabbit heart.

2. If LVH-induced modulation of repolarization $K^+$ currents were due to chronic activation of the $\alpha_1$-adrenergic receptor, then the response to acute *in vitro* administration of the selective $\alpha_1$-adrenergic agonist, methoxamine, would differ in control versus hypertrophied rabbits.

## 2.1 The Model

This is the conceptual model that will be evaluated in this project to deduce the possible mechanistic interactions that occur in pressure-overload induced LVH.

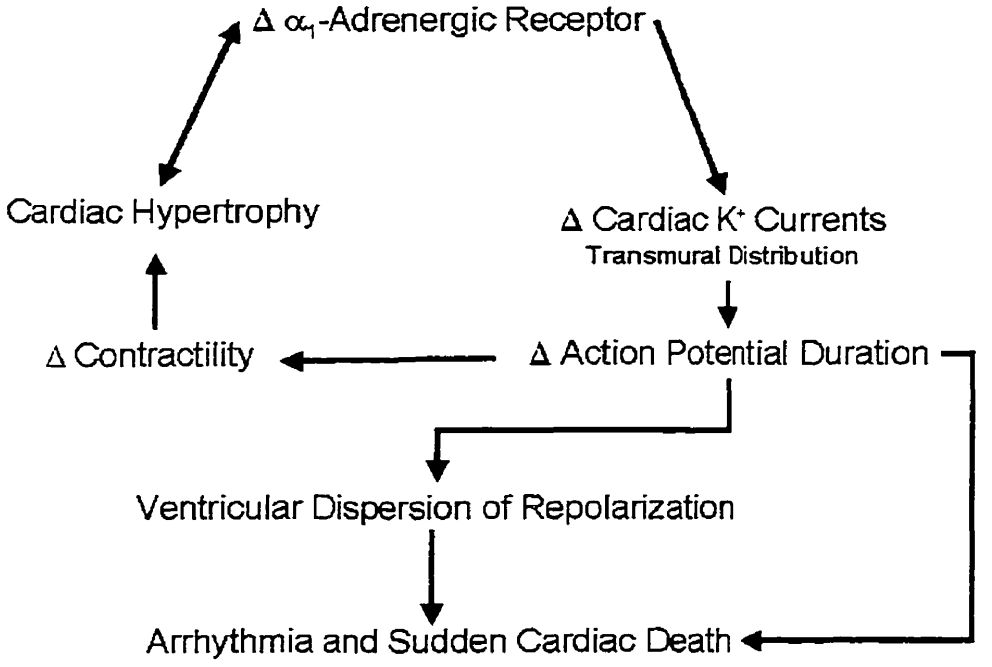

# Materials and Methods : Chapter 3

## 3.1 Rationale for the Rabbit Model

Giles *et al.,* described the various repolarization $K^+$ currents in rabbit atrial and ventricular myocytes (Giles *et al.,* 1988). They found that the rabbit contained similar cardiac repolarizating $K^+$ currents as humans (ie: predominantly $I_{to}$ and $I_{K1}$ with small $I_{Kr}$). Due to the similarities in the kinds of repolarization $K^+$ currents found in rabbits and humans, the rabbit model is a good model to study for cardiac $K^+$ current electrophysiology. In addition, a successful rabbit model of LVH was developed in the laboratory of Dr. Anne Gillis to assess the electrophysiological characteristics of pressure overload-induced cardiac hypertrophy. This surgical method (which is described in detail below) for developing LVH has been successful with other animal models in producing pressure overload-induced cardiac hypertrophy (Randhawa *et al.,* 1992) and is used in conjunction with experimentally-induced aortic insufficiency for the study of chronic heart failure (Bril *et al.,* 1991). In terms of size, rabbits are small enough to handle, but large enough to obtain accurate electrophysiological measurements of transmural distributions of cardiac $K^+$ currents.

## 3.2 Development of Left Ventricular Pressure Overload-Induced Cardiac Hypertrophy

The surgical procedure for aortic banding to develop pressure overload-induced cardiac hypertrophy is described by Gillis *et al.,* 1998. Male New Zealand White rabbits weighing 2.5 to 3.0kg were used in the surgery. The weight was chosen to ensure a low mortality rate due to the surgical procedure. Left ventricular pressure overload was induced by partial ligation of the abdominal aorta. The rabbits were randomly assigned to two groups, AS (Aortic Stenosis) and age-matched controls. Only the AS group underwent surgery. Previous studies on this model have used sham-operated controls, however the electrophysiology of these controls were no different from age-matched controls without surgery. Therefore, this surgical intervention of sham-operated controls would have been of no benefit. The night of the surgery, the rabbits were fasted. On the day of the surgery, the rabbits were sedated with acepromazine (1.0-1.5 mg/kg) administered i.v. General anesthesia was then induced with an oxygen/halothane (2.5%) mixture administered via an anesthesia mask at a rate of 1L/min. The abdominal aorta was exposed just above the renal arteries, but below the mesenteric artery. The suture was tied against a 2.1mm diameter probe, which was then withdrawn. The incision was then closed, and the animals were kept in the animal care center until the day of the study. 4 to 5 days before the study, the animals were sedated with diazepam. A 22-gauge catheter was inserted percutaneously into an ear artery for determination of the arterial blood pressure. Following the blood pressure measurement, the catheter

was then removed. These AS rabbits were kept 104±36* days post-operation before being used for electrophysiological studies. All procedures conformed to the guiding principles of the Canadian Council on Animal Care.

## PHYSIOLOGIC MECHANISM BEHIND THE MODEL

The aortic banding induces LVH in this model in two ways, the first being the actual physical restraint the banding puts on the afterload itself. By causing an aortic stenosis (AS), the immediate effect is an increase in arterial blood pressure proximal to the aortic band. The heart must pump the same volume of blood through a smaller opening than before. This increases the afterload on the heart dramatically. Alone, this stress on the heart would eventually lead to LVH. However in this model, there is another factor that adds even more stress on the heart. The fact that the banding was placed supra-renally was a very important determinant in the development of LVH in this model. The kidneys "thought" that there was a loss in arterial blood pressure because the banding reduced the amount of blood being shunted to the kidneys. In reaction to the apparent fall in arterial blood pressure, the kidneys released renin. Renin is a small protein enzyme which acts on angiotensinogen and converts it to angiotensin I. angiotensin I is converted to Angiotensin II by an enzyme produced in the lungs called angiotensin converting enzyme (ACE). Angiotensin II is a very potent vasoconstrictor, which has a two-fold effect on arterial blood pressure. It vasoconstricts the arterioles which increases peripheral resistance and thus

---

* Data shown mean±SE

increasing arterial blood pressure. In addition, angiotensin II decreases the excretion of both salt and water. This increases extracellular fluid volume, which in turn increases arterial blood pressure as well. These two effects of aortic banding result in a large increase in arterial blood pressure, which result in the pressure overload that induces LVH.

## 3.3 Ventricular Myocyte Isolation

SOLUTIONS

Solutions for myocyte isolation and the whole-cell voltage clamp studies were made using millipore-filtered water. The modified extracellular Tyrode's solution used to isolate the myocytes consisted of (mM): NaCl 130, KCl 5.5, $MgCl_2$ 0.8, $NaH_2PO_4$ 1.0, glucose 10, HEPES 10, and pH adjusted to 7.4 with NaOH. The KB solution consisted of (mM): KCl 40, $KH_2PO_4$ 20, $MgCl_2$ 5.0, $KHCO_3$ 0.5, potassium glutamate 50, potassium aspartate 20, ethyleneglycol-bis-(β-aminoethylether) N,N,N',N'-tetraacetic acid (EGTA) 0.1, glucose 10, HEPES 10, taurine 20, bovine serum albumin 0.02%, and pH adjusted to 7.4 with KOH. The HEPES-buffer solution consisted of (mM): NaCl 130, KCl 5.5, $MgCl_2$ 0.8, $CaCl_2$ 2, HEPES 10, glucose 10, and pH adjusted to 7.4 with NaOH. The internal pipette solution consisted of (mM): potassium aspartate 110, $Na_2ATP$ 4, $MgCl_2$ 4, $CaCl_2$ 1, KCl 10, EGTA 10, HEPES 5, and pH adjusted to 7.2 with KOH.

ISOLATION PROCEDURE

Single ventricular myocytes were isolated using a modified Langendorff technique (Wang *et al.,* 1996). On the day of the study, the rabbits were pretreated with heparin sulfate (75 U/kg) to reduce the amount of blood clotting once the heart was removed. The reduction of clotting allowed the blood to be washed out easily by the perfusate. The animals were then anesthetized with sodium pentobarbital

(35mg/kg). The hearts were then rapidly removed through a median sternotomy incision and perfused retrogradely via the aorta. The hearts were perfused with the Tyrode's solution (containing 2mM $CaCl_2$, pH 7.4, 37°C) for 5 minutes and then perfused with $Ca^{2+}$-free Tyrode's (containing 0.6mM EGTA) for 5 minutes. The hearts were then perfused with Tyrode's solution containing 30μM $CaCl_2$, 20U/ml of Worthington collagenase and 0.01% bovine serum albumin for 12-15 minutes. The hearts were then taken down from the Langendorff apparatus and the aorta and atria were cut from the ventricles. The ventricles were quickly weighed and the left ventricle was dissected free. The papillary muscles were removed at their base and discarded. The left ventricle was cut in half horizontally. The ventricular tissue closest to the base of the heart was then further dissected. Using a scalpel, the epicardium (1mm thick) was dissected free and cut into smaller pieces for further digestion. With the same procedure, the endocardium (1mm thick) was also dissected free. The pieces of endocardium and epicardium were incubated at 37°C with gentle agitation for 15 to 25 minutes in separate small vessels containing the modified $Ca^{2+}$-free Tyrode's solution with 121U/ml of Worthington collagenase and 0.01% bovine serum albumin. The resulting cell suspensions were then filtered through a fine-pore nylon mesh to remove large remnants of tissue and diluted (1:1) in Tyrode's solution containing 100μM $CaCl_2$ and 20% bovine serum albumin to screen for Calcium tolerance and to neutralize the collagenase. The cell suspension was allowed to passively pellet for 20 minutes at room temperature. The supernatant was carefully removed and the pellet was resuspended in KB solution. The cell suspension was then incubated at 4°C for at least 1 hour before the cells were used

for voltage clamp experiments. In some cases, the cells were left overnight at 4°C and used the next day for experiments. This protocol consistently yielded calcium tolerant ventricular myocytes that were 60 to 65% viable.

## 3.4 Whole Cell Voltage Clamp

Whole cell $K^+$ currents were recorded with an Axopatch 200 amplifier (Axon Instruments, Foster City, CA). The recording micropipettes used had tip resistances of 1 to 4MΩ when filled with the internal solution. A liquid-junction potential of approximately +10mV arose from the use of potassium aspartate in the recording micropipettes, so all membrane potential measurements were corrected by this amount. Rabbit ventricular myocytes were superfused with oxygenated HEPES-buffered solution at 37°C. $CdCl_2$ (300μM) was added to all whole cell voltage-clamp experiments to block the L-type $Ca^{2+}$ channel. For the acute methoxamine studies, 1μM propranolol (β-adrenergic receptor antagonist) was added to block any β-adrenergic effects that might interfere with the study. The cell capacitance and series resistance were measured and calculated from uncompensated capacity current transients elicited by a 10mV depolarizing voltage step from a holding potential of –80mV. The series resistance was checked regularly to ensure that there were no variations with time. During the whole cell voltage clamp studies, series resistance ($R_s$) compensation was used, however only 40% compensation was obtained. The membrane currents were monitored on a storage oscilloscope, digitized and stored on a Windows-compatible PC. Data acquisition was performed using a TL-1 DMA interface and pCLAMP software (Axon Instruments, Foster City, CA). All voltage

clamp experiments were done at 36.5±0.5°C. The rationale for using this temperature was two fold. The first is that 37°C is the physiologic temperature and thus it would make sense to record ionic currents at this temperature to obtain the most physiologically relevant measurements of the ionic currents being studied. The second is that certain ionic current characteristics can only be seen at 37°C. For example, preliminary recordings of $I_K$ currents (data not shown) at room temperature did not yield any tail currents. However, once the temperature of the bath was raised to 37°C, $I_K$ tail currents were consistently seen and recorded. In addition, kinetic measurements of $I_{to}$ would be different at room temperature compared to 37°C since kinetics are temperature dependent. At room temperature, the kinetics would be consistently slower than at 37°C.

## 3.5 Statistical Analysis

All data are presented as mean±SD unless stated otherwise. Differences between groups were compared using an unpaired Student's *t* test. Differences were considered statistically significant when $p<0.05$. Statistical analyses were done using SigmaStat (SPSS Inc. Chicago, Il).

# Results : Chapter 4

## 4.1 Indices of Hypertrophy

In determining the effectiveness of our model of left ventricular pressure overload-induced cardiac hypertrophy (LVH), a set of measurements or indices were used to measure the level of hypertrophy. The indices measured for this project were blood pressure (BP), heart wet weight to body weight ratio (HW/BW), and cell ventricular capacitance (measure of cell size). Table 1 summarizes the results obtained for the indices measured. Systolic BP for AS rabbits was 35% greater than controls and the diastolic BP was 30% greater. In the endocardium, the cell capacitance was 19% greater in AS compared to controls. In the epicardium, the cell capacitance was 18% greater in AS compared to controls. In addition, AS rabbit HW/BW was significantly larger than control values, suggesting that the AS rabbit heart was hypertrophic. Based on the above indices of hypertrophy, it can be concluded that the surgical technique used in this project was effective in creating LVH.

**Table 1. Effect of Suprarenal Aortic-banding on Indices of Cardiac Hypertrophy**

| Index | Control | AS |
|---|---|---|
| **Blood Pressure (mmHg) Systole/Diastole** | 104±13/77±9 (11) | 159±20/110±14 (11)* |
| **Ventricular Cell Capacitance (pF) Endocardium** | 140±53 (113) | 173±63 (65)* |
| **Ventricular Cell Capacitance (pF) Epicardium** | 132±34 (21) | 161±29 (12)* |
| **Heart/Body Weight Ratio (g/kg)** | 3.3±0.4 (41) | 3.6±0.4 (26)* |

Values are expressed as mean±SD. Brackets indicate the number of measurements.

*$p<0.05$ as compared to Controls by an unpaired *t* test.

## 4.2 Changes in the Depolarization-Activated Outward $K^+$ Current

### TRANSIENT OUTWARD $K^+$ CURRENT ($I_{to}$) DENSITY

Fig 1 shows the effect of the $I_{to}$ blocker, 1mM 4-aminopyridine (4-AP) on the depolarization activated outward $K^+$ current. As expected, 1mM 4-AP blocked the outward $K^+$ current significantly. The effect of 4-AP was much greater on the peak of the outward current than on the sustained current. In Fig 2, the raw trace morphology of the depolarization-activated outward $K^+$ current was similar in all subgroups evaluated. However, currents from control myocytes (in both endocardium and epicardium) were larger than currents from AS myocytes. Previous studies have shown that the outward transient $K^+$ current ($I_{to}$) and the sustained current ($I_{sus}$) are components of the depolarization-activated outward $K^+$ current. $I_{to}$ can be determined by subtracting the peak outward current from the plateau current ($I_{sus}$). Fig 3 shows the Current-Voltage (IV) relationships of $I_{to}$ among the groups studied. Panel A showed no significant differences between $I_{to}$ current density in control endocardium (n=33) and epicardium (n=14). Also, there were no significant changes in AS endocardium (n=31) versus AS epicardium (n=5). However, there were significant changes observed when comparing AS versus controls in both endocardium and epicardium (panel B). Interestingly, the decrease in $I_{to}$ current density at +40mV was more pronounced in the epicardium (35±8%) than in the endocardium (18±6%) ($p<0.05$).

## $I_{sus}$ DENSITY

Fig 4 shows the IV relationships of $I_{sus}$ among the subgroups studied. Again, panel A shows no significant differences in $I_{sus}$ current density in control endocardium (n=33) versus epicardium (n=14). Also, there were no significant changes in AS endocardium (n=31) versus epicardium (n=5). However, there were significant changes when comparing AS versus controls in the epicardium (panel B) ($p<0.05$). LVH decreased $I_{sus}$ by 21% compared to controls. In contrast, LVH had no effect on $I_{sus}$ current density in the endocardium. In summary, the current density of $I_{to}$ and $I_{sus}$ were decreased by LVH and that decrease was regionally dependent.

## $I_{to}$ KINETIC STUDIES

### INACTIVATION

Fig 5 shows that $I_{to}$ inactivation best fits a bi-exponential function. This suggests that $I_{to}$ was comprised of two components: Fast and Slow. The equation of this bi-exponential function is as follows:

$$I_{to}=A_o-A_1^{(-t/\tau f)}+A_2^{(-t/\tau s)} \quad \text{equation 1}$$

$A_o$ is a constant, $A_1$ and $A_2$ are the amplitudes of the fast and slow components, respectively, of $I_{to}$, t is the time elapsed and $\tau_f$ and $\tau_s$ are the fast and slow time constants of inactivation, respectively (Meszaros *et al.*, 1996). In the endocardium (Fig 6 panel A) there were no significant differences in the $\tau$/Voltage relationship in

control (n=6) versus AS (n=7) for both $\tau_f$ and $\tau_s$. Similarly, in the epicardium (panel B) there were no significant differences in the $\tau$/Voltage relationship in control (n=6) versus AS (n=4) for both $\tau_f$ and $\tau_s$. Fig 6 shows that $I_{to}$ inactivation rates were voltage-independent.

STEADY STATE INACTIVATION

Fig 7 and 8 show the representative raw traces and mean steady-state inactivation relationships (shown as fits to a cumulative Boltzmann distribution) of $I_{to}$ respectively. Fig 8 panel A shows no significant changes in mean $I_{to}$ steady-state inactivation in control endocardium (n=3, $V_{1/2}$= -0.6±0.6mV, Slope= -4.3±0.6mV$^{-1}$)* versus epicardium (n=5, $V_{1/2}$= -3.5±0.6mV, Slope= -4.1±0.5mV$^{-1}$)*. Also, there were no significant changes in AS endocardium (n=3, $V_{1/2}$= 0.8±1.1mV, Slope= -7.5±0.9mV$^{-1}$)* versus epicardium (n=4, $V_{1/2}$= -1.8±0.5mV, Slope= -3.8±0.4mV$^{-1}$)*. In panel B, there were no significant differences in control versus AS in both endocardium and epicardium. These observations suggested that the inactivation properties of $I_{to}$ are not altered by LVH in different regions of the heart.

* Data shown mean±SE

Fig 1 **The depolarization-activated outward $K^+$ current was blocked by the $I_{to}$ blocker, 4-aminopyridine (4-AP).** Representative examples of the depolarization activated outward $K^+$ current measured at (**A**) baseline and in the presence of (**B**) 1mM 4-AP. In addition, at the concentration measured, there was a much greater 4-AP block at the peak of the outward current than at the steady state. In keeping with previous literature, the peak outward current was 4-AP sensitive.

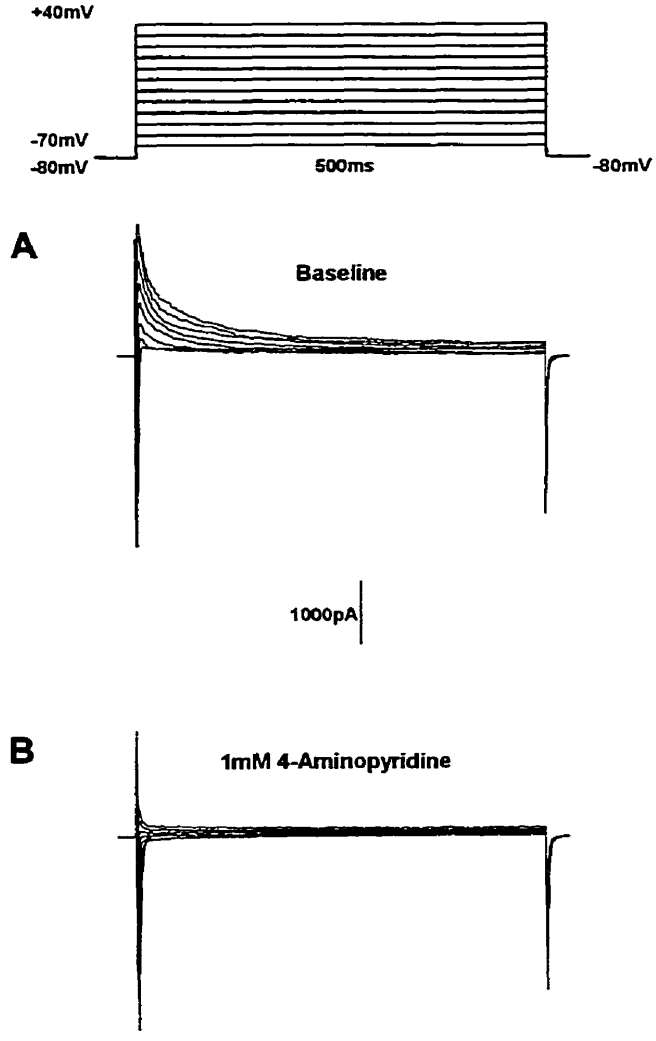
+40mV
-70mV
-80mV
500ms
-80mV
A
Baseline
1000pA
B
1mM 4-Aminopyridine

Fig 1

Fig 2 **Representative traces of current density of the depolarization-activated outward $K^+$ current** recorded from endocardial (**A** and **C**) and epicardial myocytes (**B** and **D**) from control and AS rabbits. Currents were elicited using the protocol inset shown in Fig 1.

Fig 2

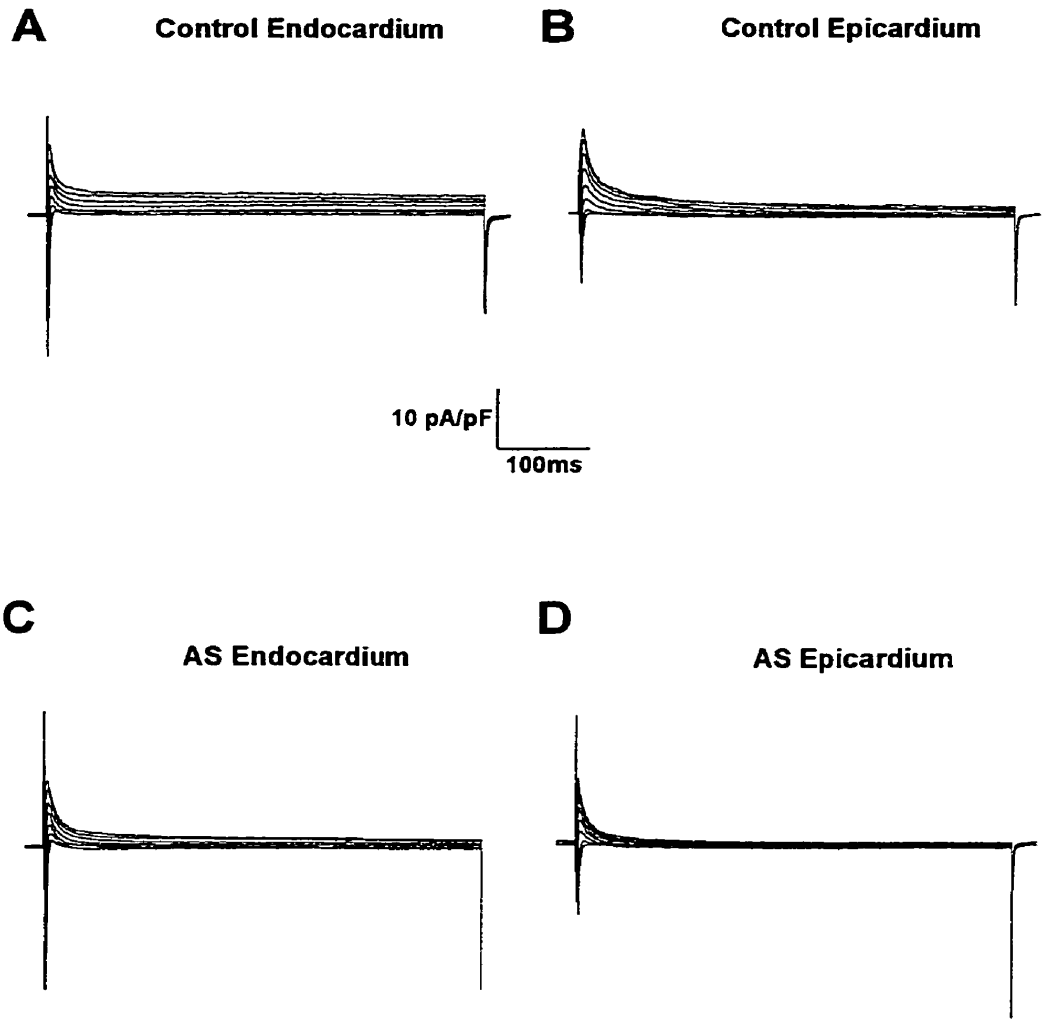
A
Control Endocardium
B
Control Epicardium
10 pA/pF
100ms
C
AS Endocardium
D
AS Epicardium

Fig 3 **$I_{to}$ was significantly decreased in AS compared to controls.** $I_{to}$ was determined by subtracting the $I_{sus}$ (sustained current) from the peak outward current. Currents were measured at the peak of the outward current. (**A**) Mean IV relationships comparing endocardial (**circles**) versus epicardial (**squares**) myocytes in control (**closed**) and AS (**open**) rabbits. There were no differences in $I_{to}$ current density between endocardial and epicardial myocytes in both control and AS. (**B**) Mean IV relationships comparing control versus AS myocytes in the endocardium and epicardium. There was a significant decrease in $I_{to}$ current density in AS compared to control in both the endocardium and epicardium. However, the decrease in $I_{to}$ was significantly greater in the epicardium than in the endocardium. Values shown as mean±SD. (*) Represents statistical significance with a $p<0.05$ as determined using an unpaired Student's *t* test. (**NS**) Represents non-significance. See text for n values.

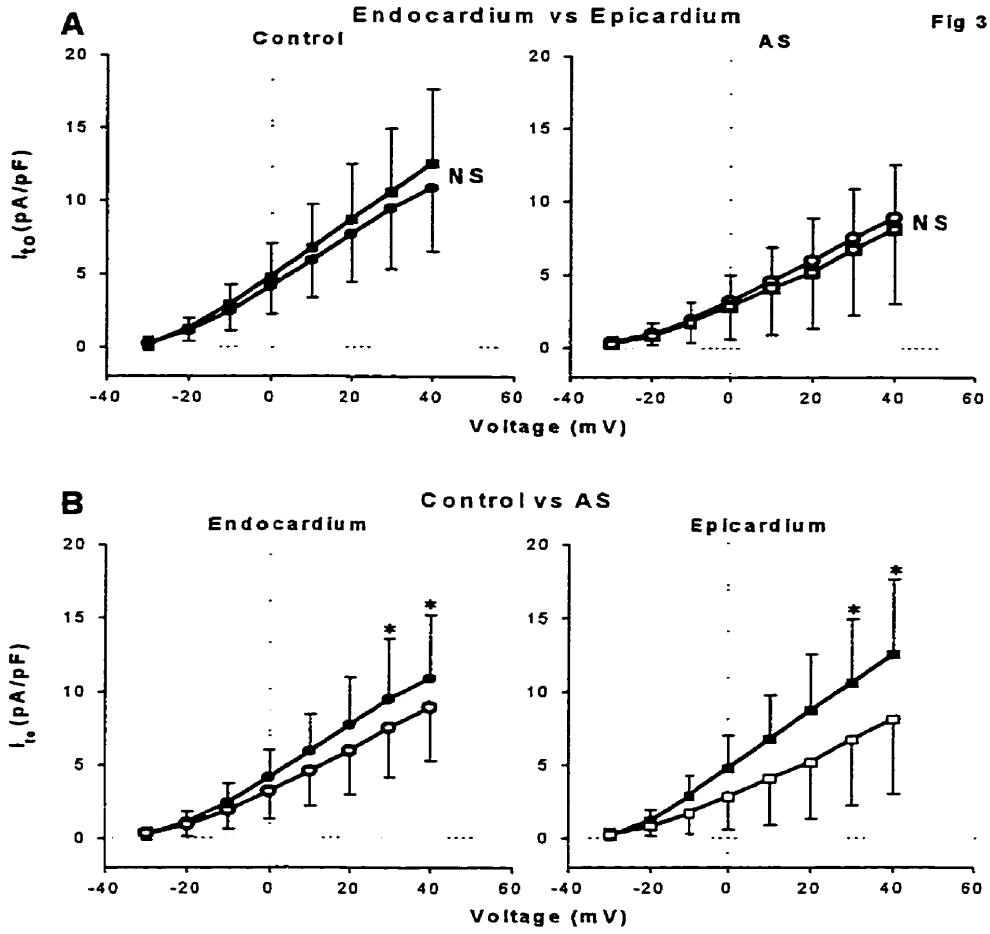
A
Endocardium vs Epicardium
Control
AS
NS
NS
$I_{to}$ (pA/pF)
Voltage (mV)
B
Control vs AS
Endocardium
Epicardium
$I_{to}$ (pA/pF)
Voltage (mV)

Fig 3

Fig 4 **$I_{sus}$ was significantly decreased in AS epicardial myocytes compared to control**. Currents were measured at the end of the 500ms pulse where the current reached steady state. **A)** Mean IV relationships comparing endocardial (**circles**) versus epicardial (**squares**) myocytes in control (**closed**) and AS (**open**) rabbits. There were no differences in $I_{sus}$ current density between endocardial and epicardial myocytes in both control and AS. (**B**) Mean IV relationships comparing control versus AS myocytes in the endocardium and epicardium. There was a significant decrease in $I_{sus}$ current density in AS compared to control in the epicardium, but not in the endocardium. Values shown as mean±SD. (*) Represents statistical significance with a $p<0.05$ as determined using an unpaired Student's *t* test. (**NS**) Represents non-significance. See text for n values.

Fig 4

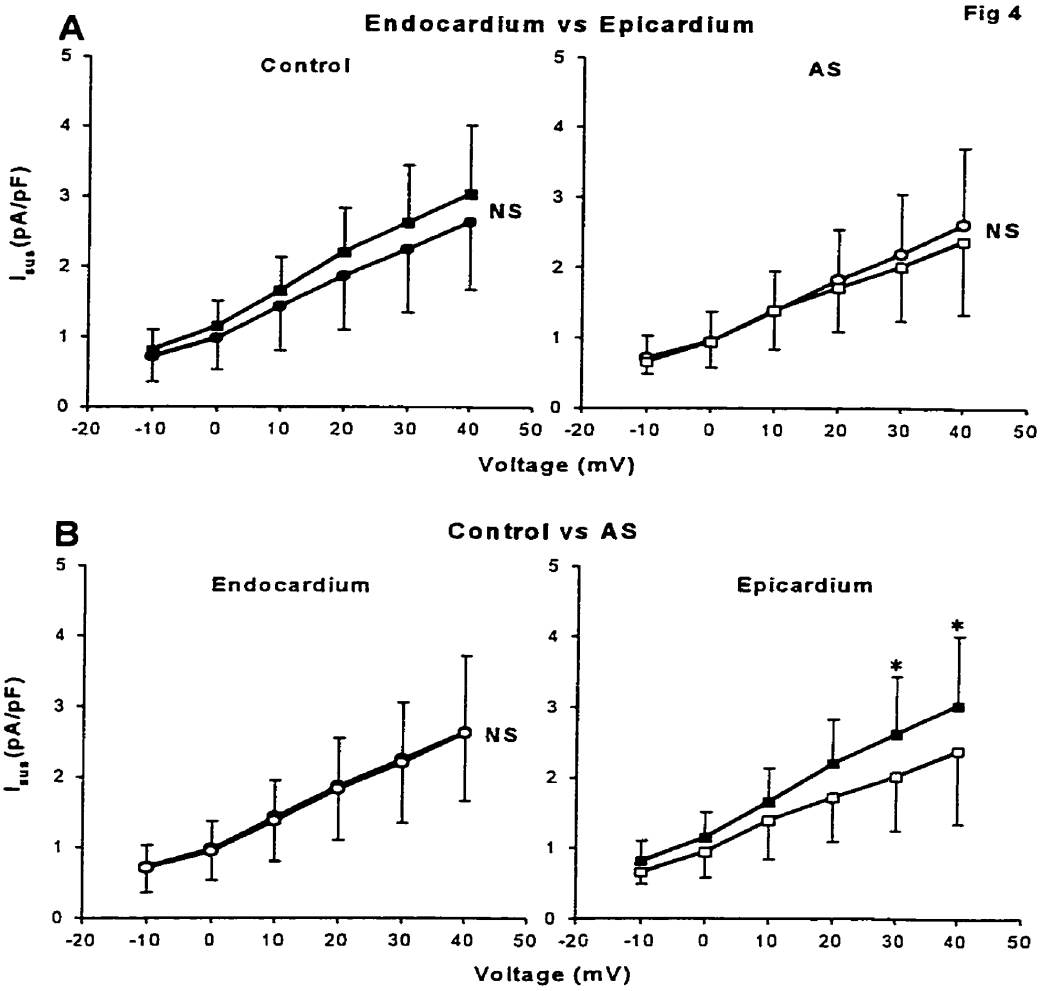
A
Endocardium vs Epicardium
Control
AS
NS
NS
$I_{sus}$ (pA/pF)
Voltage (mV)
B
Control vs AS
Endocardium
Epicardium
NS
*
*
$I_{sus}$ (pA/pF)
Voltage (mV)

Fig 5 **Representative mono- and bi-exponential fitting of the depolarization-activated outward $K^+$ current inactivation in control endocardial myocytes.** (**A**) Mono-exponential fit (**Solid line**) superimposed on the raw current trace (**Dashed line**) measured at +40mV. (**B**) Bi-exponential fit. The figure shows that the depolarization-activated outward $K^+$ current inactivation was not well fit to a mono-exponential, but was well fit to a bi-exponential. The depolarization-activated outward $K^+$ current comprised a fast and a slow component.

Fig 5

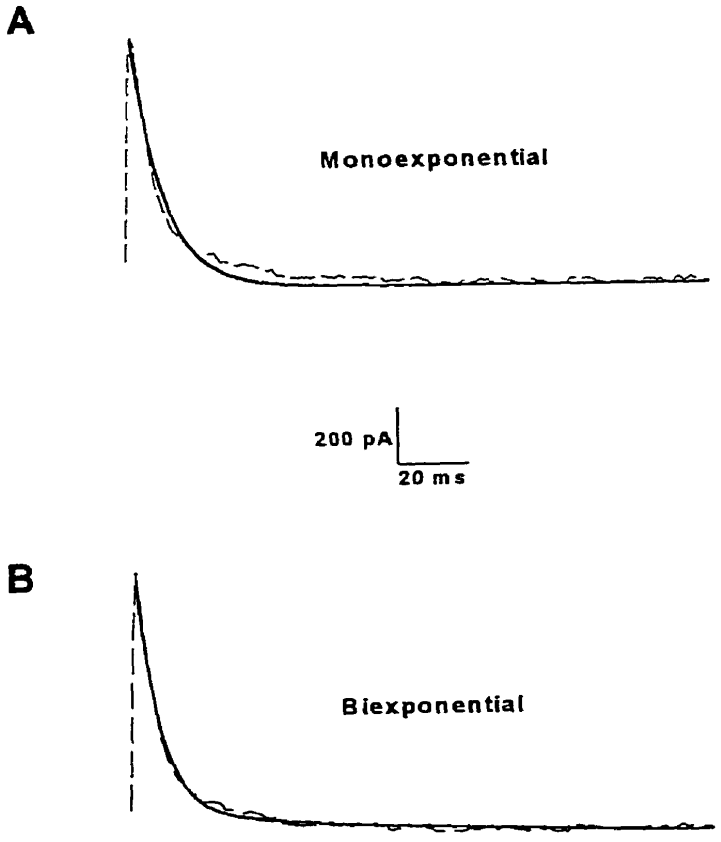

Fig 6 **The depolarization-activated outward $K^+$ current inactivation process was voltage independent.** Currents were fit to a bi-exponential model and had fast and slow time constants (Tau) that were derived from equation 1 from the text. (**A**) Mean relationships between Tau and voltage comparing controls (**closed**) versus AS (**open**) in the endocardium. Neither the fast nor slow Tau showed any voltage dependence in the endocardium. (**B**) Mean relationships between Tau and voltage comparing controls versus AS in the epicardium. Neither the fast nor slow Tau showed any voltage dependence in the epicardium. Values shown as mean±SD. See text for n values.

Fig 6

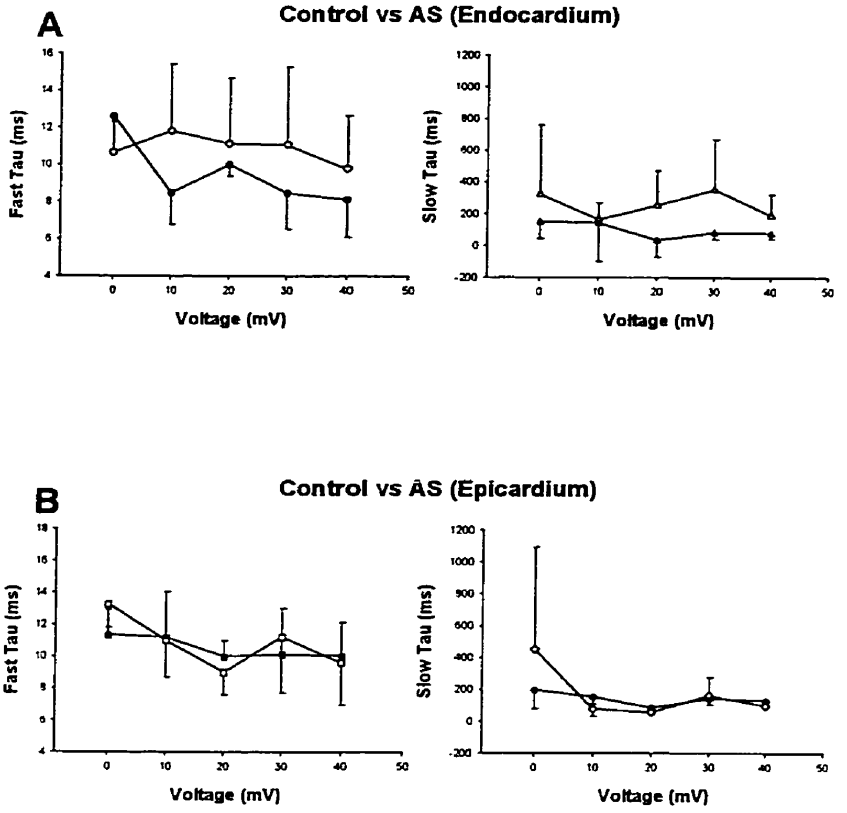
A
Control vs AS (Endocardium)
Fast Tau (ms)
Slow Tau (ms)
Voltage (mV)
Voltage (mV)
B
Control vs AS (Epicardium)
Fast Tau (ms)
Slow Tau (ms)
Voltage (mV)
Voltage (mV)

Fig 7 **Representative examples of recordings showing steady-state inactivation of $I_{to}$** recorded from endocardial (**A** and **C**) and epicardial (**B** and **D**) myocytes from control and AS rabbits.

Fig 7

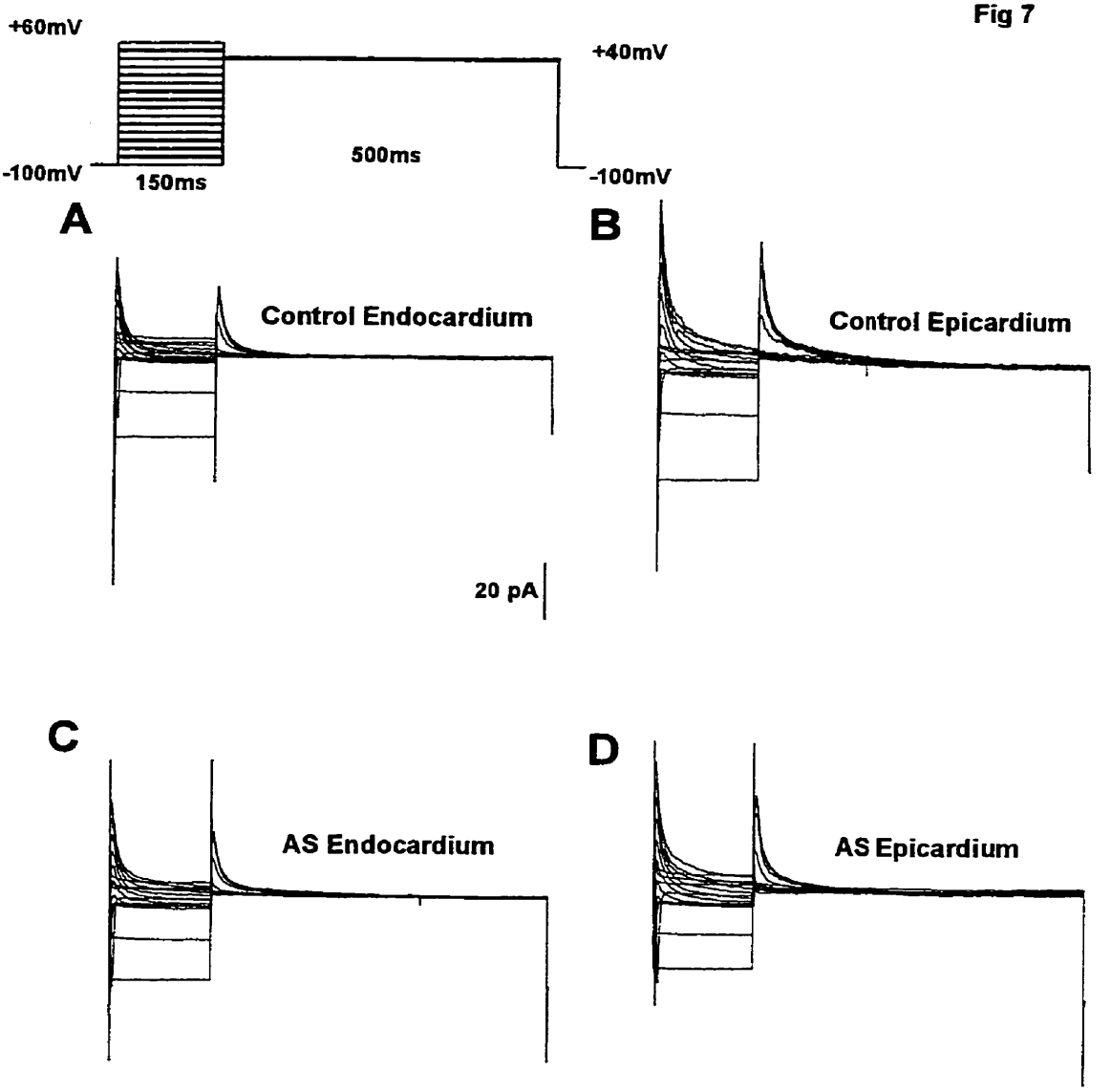
+60mV
-100mV
150ms
500ms
+40mV
-100mV
A
Control Endocardium
20 pA
B
Control Epicardium
C
AS Endocardium
D
AS Epicardium

Fig 8 **No differences in $I_{to}$ steady state inactivation between control and AS or between endocardium and epicardium.** Currents were measured at the peak of the current elicited by the 500ms +40mV pulse. (**A**) Mean steady state inactivation relationships comparing endocardial (**circles**) versus epicardial (**squares**) myocytes in control (**closed**) and AS (**open**) rabbits. There were no significant differences in $I_{to}$ steady state inactivation parameters ($V_{1/2}$ and the slope factor) in endocardial versus epicardial myocytes in both controls and AS. Values for $V_{1/2}$ and slopes are given in the text. (**B**) Mean steady state inactivation relationships comparing control versus AS myocytes in the endocardium and epicardium. There were no significant differences in $I_{to}$ steady state inactivation parameters in AS compared to control in both the endocardium and epicardium. Values for $V_{1/2}$ and slopes are given in the text. Values shown as mean±SD. See text for n values.

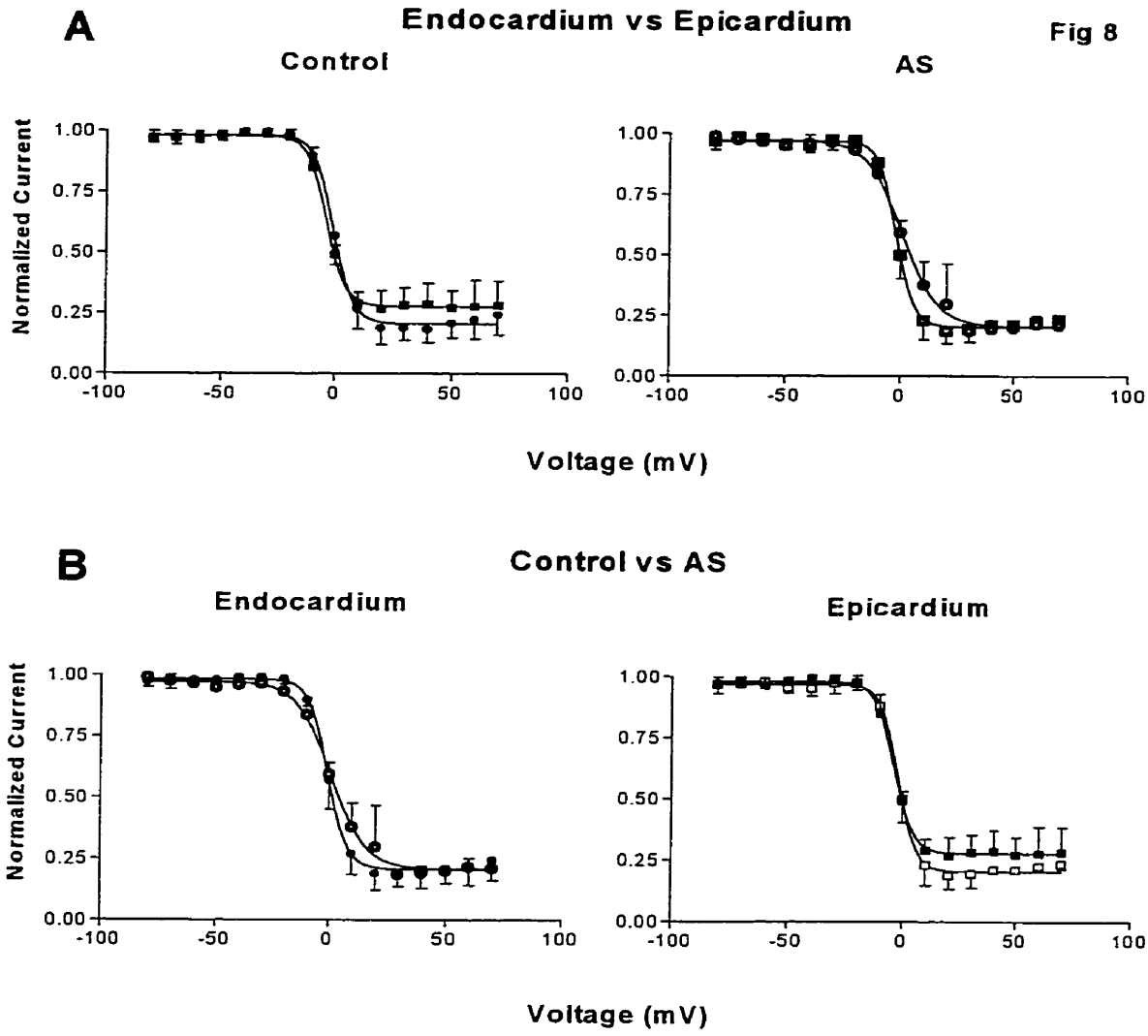
A
Endocardium vs Epicardium
Fig 8
Control
AS
Normalized Current
1.00
0.75
0.50
0.25
0.00
-100
-50
0
50
100
Voltage (mV)
B
Control vs AS
Endocardium
Epicardium
Normalized Current
1.00
0.75
0.50
0.25
0.00
-100
-50
0
50
100
Voltage (mV)

## 4.3 Changes in the Inwardly Rectifying $K^+$ Current, $I_{K1}$

Fig 9 shows the effect of the $I_{K1}$ blocker, 50μM barium chloride, on the inwardly rectifying $K^+$ current, $I_{K1}$. As expected, external barium blocked the inwardly rectifying $K^+$ current significantly. Fig 10 and 11 show the representative raw traces and mean IV relationships of $I_{K1}$ respectively. Fig 11 panel A shows no significant differences in $I_{K1}$ current density in control endocardium (n=78) compared to epicardium (n=19). Also, in AS animals, there were no significant differences between endocardium (n=60) and epicardium (n=12). However, there were significant changes observed when comparing control versus AS in the endocardium (Fig 11B). LVH decreased both the inward and outward portions of $I_{K1}$ significantly compared to controls. In contrast, LVH had no effect on $I_{K1}$ current density in the epicardium. In summary, the current density of $I_{K1}$ was decreased by LVH and this decrease was regionally dependent.

Fig 9 **The inwardly rectifying $K^+$ current ($I_{K1}$) was blocked by the $I_{K1}$ blocker, barium chloride.** Representative examples of $I_{K1}$ currents measured at baseline (**A**) and in the presence of 50μM barium chloride (**B**). In keeping with previous literature, the inwardly rectifying current was barium chloride sensitive.

Fig 9

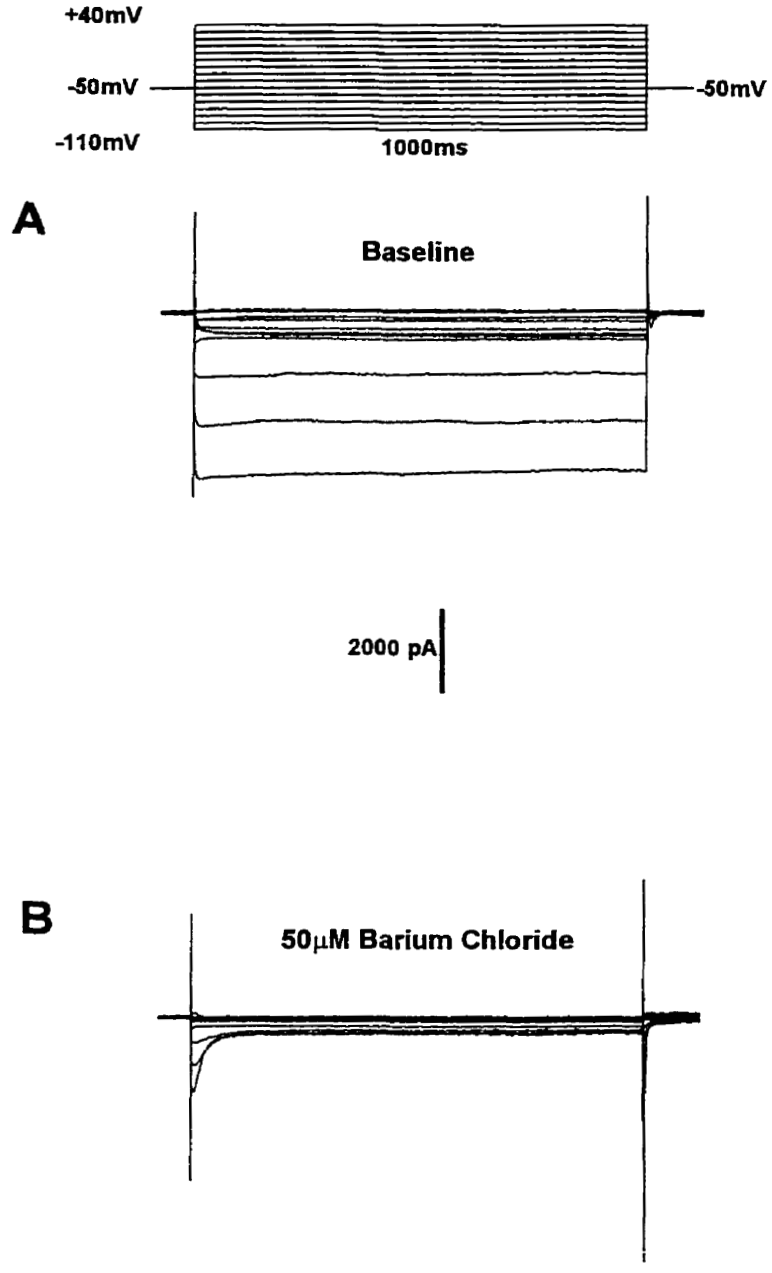
+40mV
-50mV
-110mV
-50mV
1000ms
A
Baseline
2000 pA
B
50μM Barium Chloride

Fig 10 **Representative traces of $I_{K1}$ currents** recorded from endocardial (**A** and **C**) and epicardial myocytes (**B** and **D**) from control and AS rabbits. Currents were elicited using the protocol inset shown in Fig 9.

Fig 10

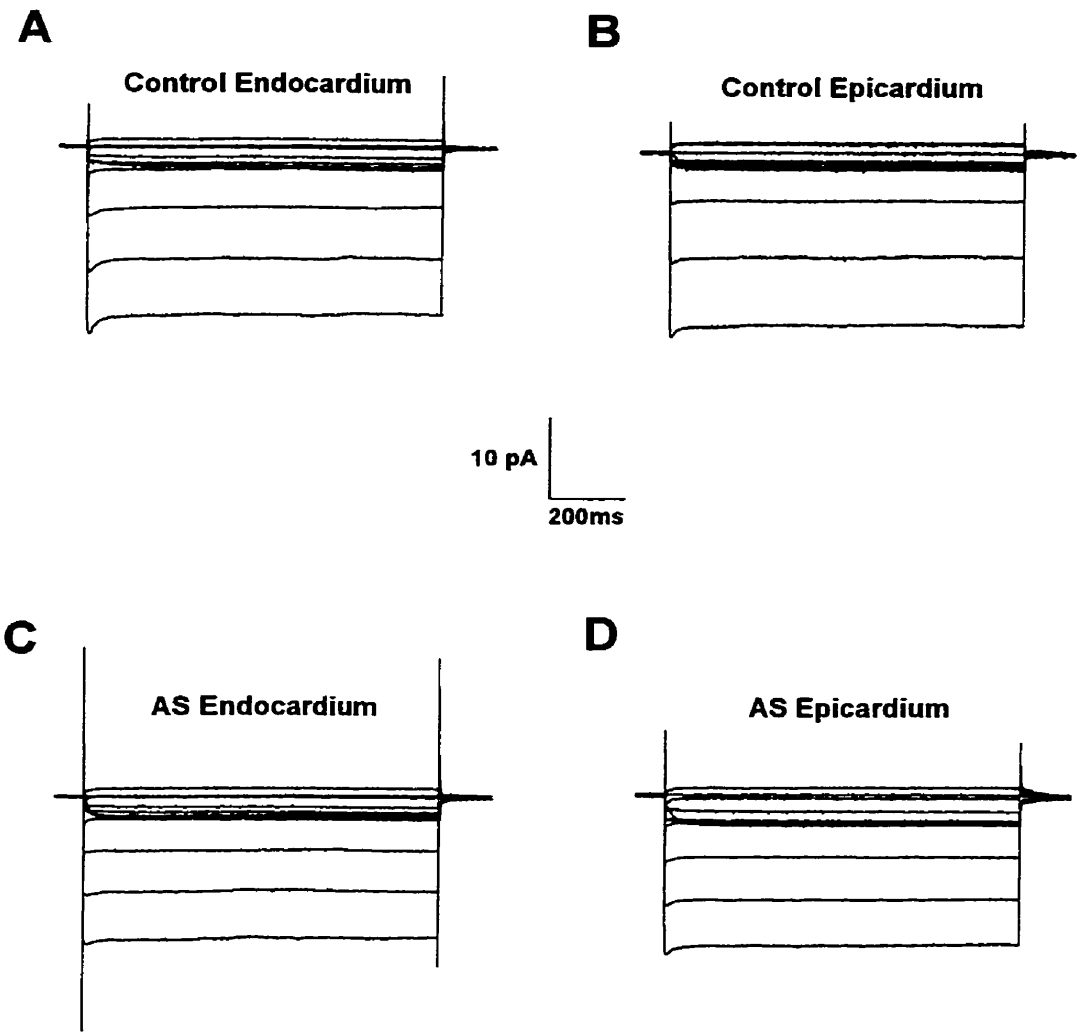
A
Control Endocardium
B
Control Epicardium
10 pA
200ms
C
AS Endocardium
D
AS Epicardium

Fig 11 **$I_{K1}$ was significantly decreased in AS endocardial myocytes compared to control, but not in epicardium.** Currents were measured at the end of the 1000ms pulse where the current reached steady state. **A)** Mean IV relationships comparing endocardial (**circles**) versus epicardial (**squares**) myocytes in control (**closed**) and AS (**open**) rabbits. There were no differences in $I_{K1}$ current density in endocardial versus epicardial myocytes in both control and AS. (**B**) Mean IV relationships comparing control versus AS myocytes in the endocardium and epicardium. There was a significant decrease in $I_{K1}$ current density at both the inward and outward portions of $I_{K1}$ in AS compared to controls in the endocardium, but not in the epicardium. The insert in graph (**B**) shows the IV relationship of the outward portion (from -70 to -40mV) of $I_{K1}$ at an increased scale. Values shown as mean±SD. (*) Represents statistical significance with a $p<0.05$ as determined using an unpaired Student's *t* test. See text for n values.

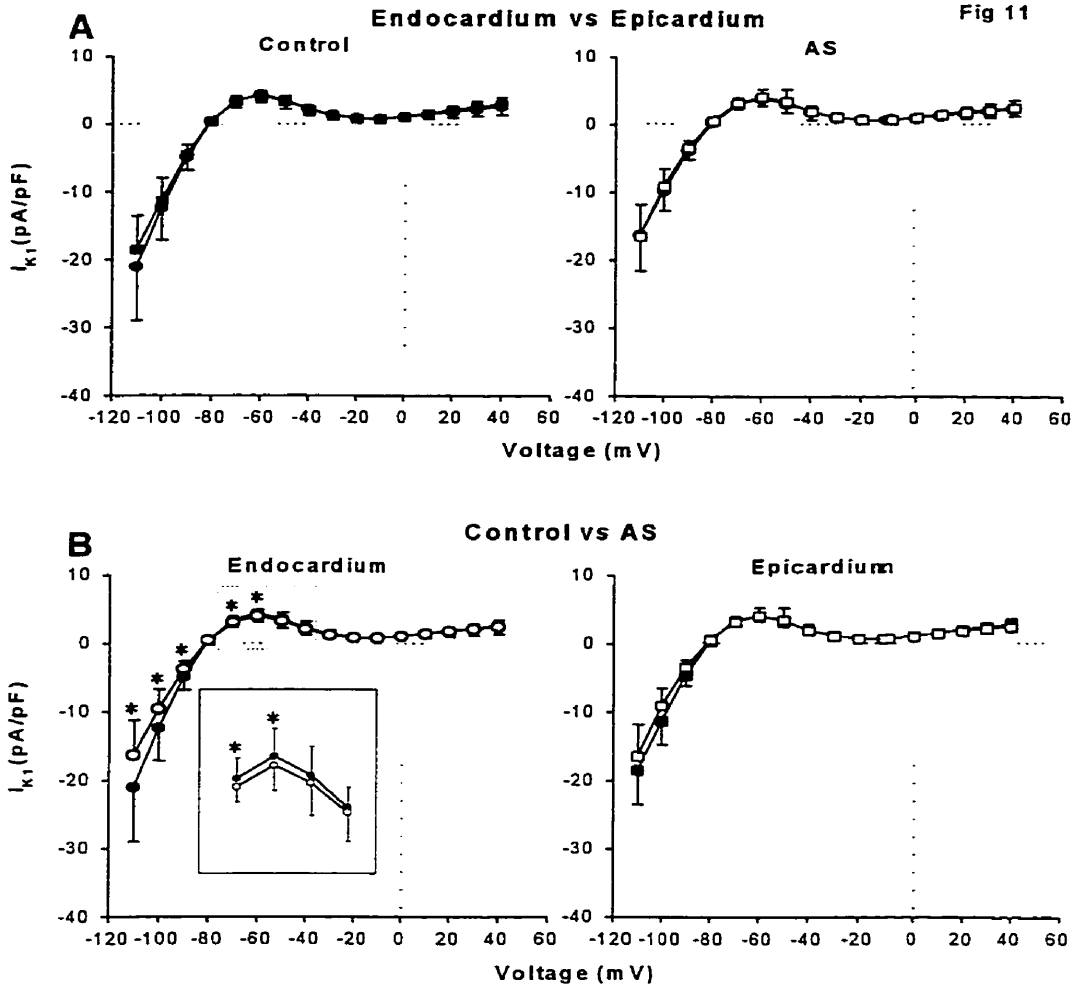
A
Endocardium vs Epicardium
Control
AS
$I_{K1}$ (pA/pF)
Voltage (mV)
B
Control vs AS
Endocardium
Epicardium
$I_{K1}$ (pA/pF)
Voltage (mV)

Fig 11

## 4.4 Changes in the Delayed Rectifying $K^+$ Current, $I_K$

Fig 12 shows the effect of the selective $I_{Kr}$ blocker, 1μM Dofetilide, on the delayed rectifying $K^+$ current, $I_K$. This concentration of dofetilide selectively blocks all of the rapid component of the delayed rectifier, $I_{Kr}$, without having any substantial effects on $I_{Ks}$. Dofetilide completely blocks the tail current of the delayed rectifying $K^+$ current. Thus, this data suggested that the tail current of $I_K$ measured in this rabbit model was predominantly comprised of $I_{Kr}$. Only the tail currents were measured and evaluated for this project. Fig 13 and 14 show the representative raw traces and mean IV relationships of $I_{Kr}$ tails respectively. Fig 14A shows that $I_{Kr}$ tail current density in control endocardium (n=20) was significantly greater than epicardium (n=18). Also, $I_{Kr}$ tail current density in AS endocardium (n=11) was significantly greater than epicardium (n=10). This suggested that there was a regional dispersion of $I_{Kr}$ from endocardium to epicardium. Also, LVH augmented the regional dispersion of $I_{Kr}$. In controls at +40mV, endocardial $I_{Kr}$ was 19% greater than epicardial $I_{Kr}$. However in AS at +40mV, endocardial $I_{Kr}$ was 27% greater than epicardial $I_{Kr}$. In contrast, there were no significant changes when comparing control versus AS in both the endocardium and epicardium (Fig 14B). In summary, the tail current density of $I_{Kr}$ showed regional dispersion between endocardium and epicardium and this dispersion was augmented by LVH.

Fig12 **The delayed rectifying $K^+$ tail current ($I_K$) was blocked by the selective $I_{Kr}$ blocker, dofetilide.** Representative examples of $I_K$ currents measured at baseline (**A**) and in the presence of 1μM Dofetilide (**B**). The tail currents were completely suppressed by dofetilide. This suggested that the delayed rectifying $K^+$ tail current was predominantly $I_{Kr}$.

Fig 12

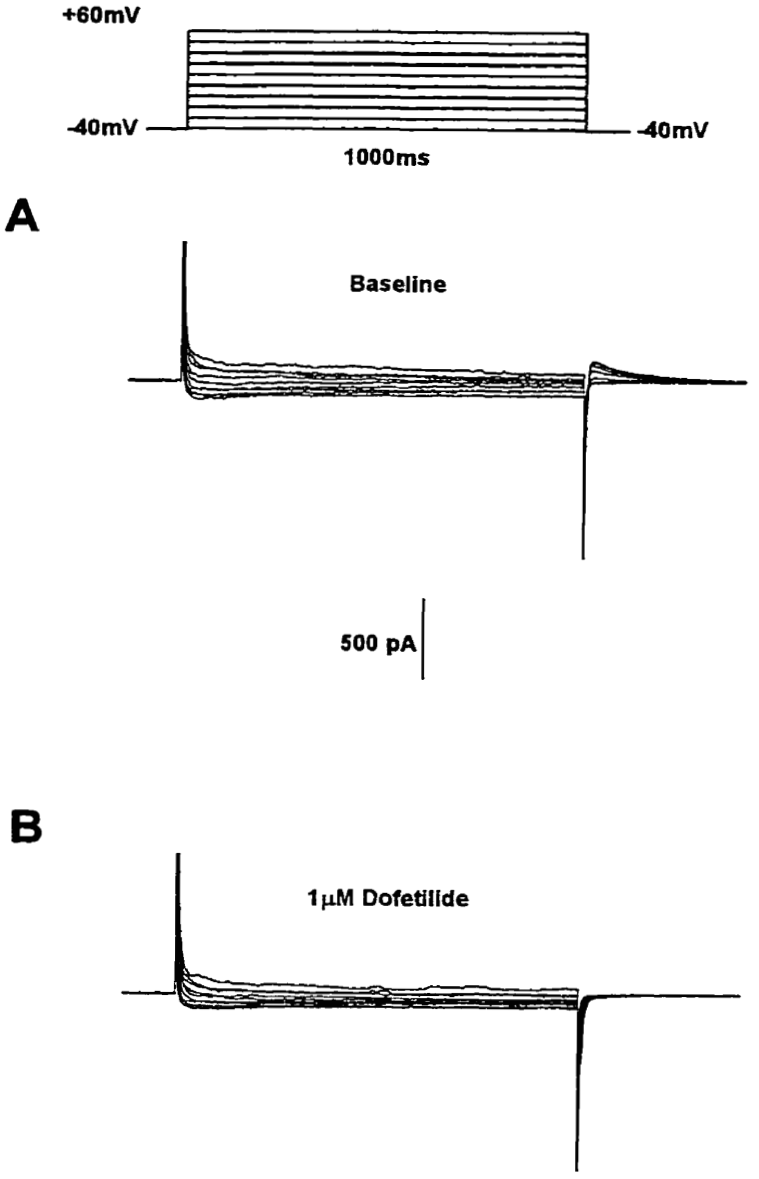

Fig 13 **Representative traces of ($I_K$) tail currents** recorded from endocardial (**A** and **C**) and epicardial myocytes (**B** and **D**) from control and AS rabbits. Currents were elicited using the protocol inset shown in Fig 12.

Fig 13

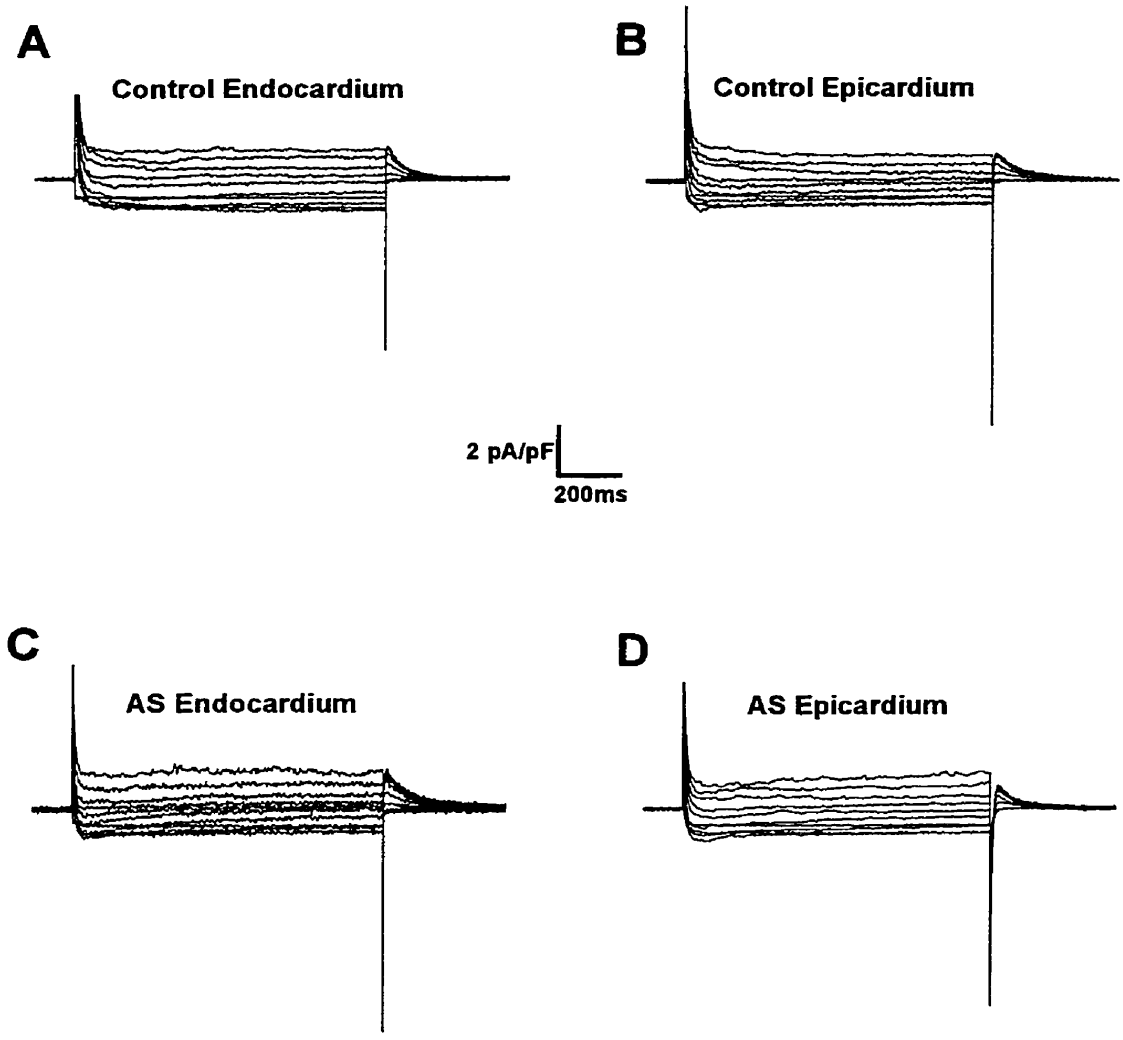
A
Control Endocardium
B
Control Epicardium
2 pA/pF
200ms
C
AS Endocardium
D
AS Epicardium

Fig 14 **$I_{Kr}$ tail currents were significantly decreased in epicardial myocytes compared to endocardial myocytes in both controls and AS.** Currents were measured at the peak of each tail current. **A)** Mean IV relationships comparing endocardial (**circles**) versus epicardial (**squares**) myocytes in control (**closed**) and AS (**open**) rabbits. $I_{Kr}$ tail current density was smaller in epicardial than in endocardial myocytes in both controls and AS. (**B**) Mean IV relationships comparing control versus AS myocytes in the endocardium and epicardium. There were no differences in $I_{Kr}$ tail current density between control and AS in either endocardium or epicardium. Values shown as mean±SD. (*) Represents statistical significance with a $p<0.05$ as determined using an unpaired Student's *t* test. See text for n values.

Fig 14

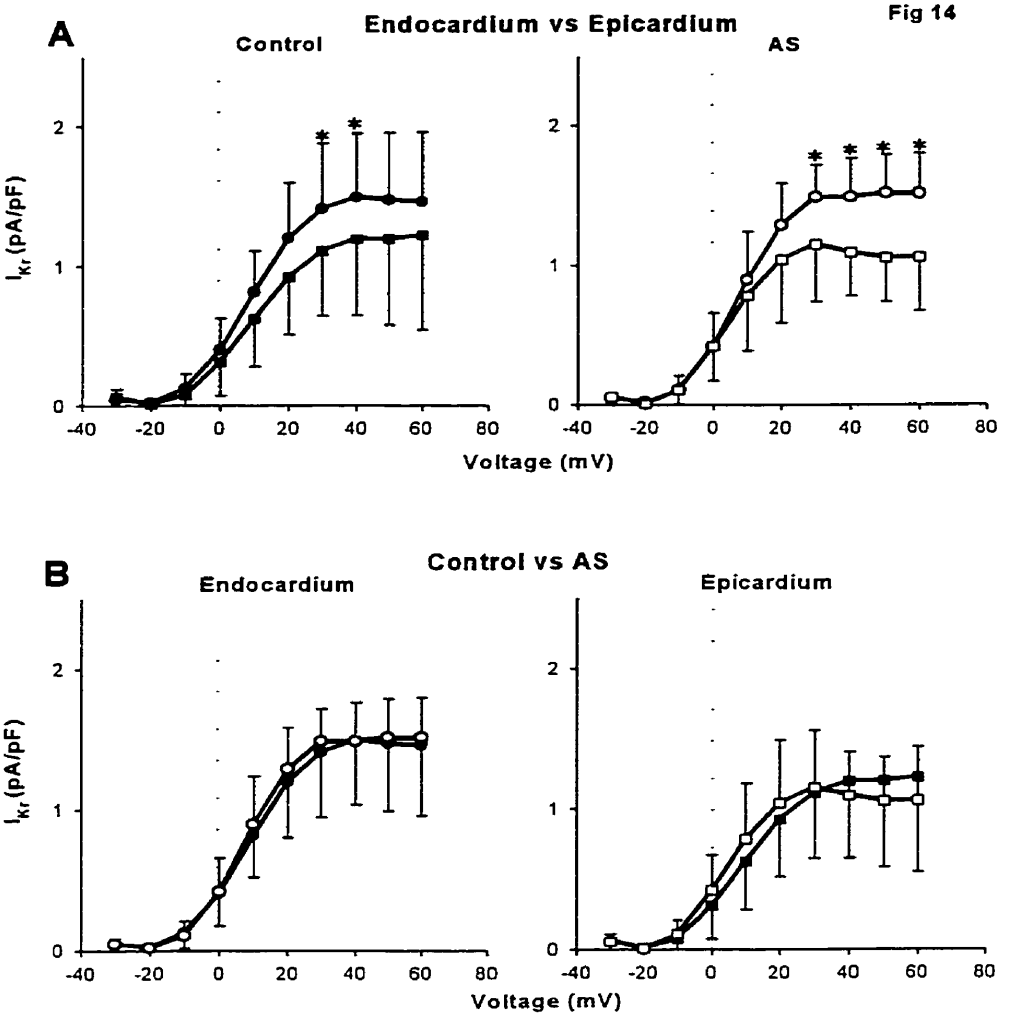
A
Endocardium vs Epicardium
Control
AS
$I_{Kr}$ (pA/pF)
Voltage (mV)
B
Control vs AS
Endocardium
Epicardium
$I_{Kr}$ (pA/pF)
Voltage (mV)

## 4.5 Effects of *in vitro* Administration of 100μM Methoxamine on $K^+$ Currents

DEPOLARIZATION ACTIVATED OUTWARD $K^+$ CURRENT

Fig 15 shows representative examples of the depolarization-activated outward $K^+$ current at baseline and in the presence of 100μM methoxamine. Methoxamine partially blocked the peak outward current, but had no significant effect on the sustained current. Also, methoxamine block of the depolarization-activated outward $K^+$ current was significantly more pronounced in control myocytes than AS myocytes. The modulatory effect of methoxamine was similar in endocardium versus epicardium for both control and AS myocytes. Table 2 showed the mean % block in each of the subgroups evaluated. These data suggested that LVH decreased the inhibitory effect of acute *in vitro* methoxamine on the depolarization-activated outward $K^+$ current, and that the effect of methoxamine was regionally-independent.

INWARDLY RECTIFYING $K^+$ CURRENT

Fig 16 shows representative examples (at –110mV and –60mV) of $I_{K1}$ at baseline and in the presence of 100μM methoxamine. Methoxamine's inhibitory effect on $I_{K1}$ was predominantly seen in the inward portion (-110mV) of the current. The outward portion of $I_{K1}$ was only marginally inhibited. Table 3 shows the mean % block in each of the subgroups evaluated. Also, the inhibitory effect of methoxamine was similar in

endocardium and epicardium. In summary, methoxamine had an inhibitory effect on $I_{K1}$ that was more easily observed for the inward portion of the current and that the effect was similar throughout all subgroups evaluated.

## DELAYED RECTIFYING $K^+$ CURRENT

Fig 17 and 18 show representative examples of $I_{Kr}$ tail currents at baseline and in the presence of 100μM methoxamine in control and AS respectively. The tail currents were marginally inhibited by methoxamine. Table 4 shows the mean % block in each of the subgroups evaluated. The inhibitory effect of methoxamine did not differ significantly between controls and AS or between endocardium versus epicardium. In summary, methoxamine had a marginal inhibitory effect of $I_{Kr}$ tail currents that was not significantly different among the subgroups evaluated.

**Table 2. $I_{to}$ Response to 100μM Methoxamine Given *in vitro***

| Model | Control | AS |
|---|---|---|
| **% Block at 40 mV Endocardium** | 49±10 (4) | 26±14 (4)* |
| **% Block at 40 mV Epicardium** | 41±14 (7) | 27±7 (5)* |

Values are expressed as mean±SD. Brackets indicate the number of cells.*$p<0.05$ as compared to Controls by an unpaired *t* test.

**Table 3. $I_{K1}$ Response to 100μM Methoxamine Given *in vitro***

| Model | Control | AS |
|---|---|---|
| **% Block at -110 and -60 mV Endocardium** | 19±20 and 4±27 (6) | 26±14 and 4±18 (5) |
| **% Block at -110 and -60 mV Epicardium** | 35±22 and 1±18 (7) | 17±17 and 1±10 (5) |

Values are expressed as mean±SD. Brackets indicate the number of cells.

Differences between controls and AS data proved to be insignificant based on an unpaired *t* test.

**Table 4. $I_{Kr}$ Response to 100μM Methoxamine Given *in vitro***

| Model | Control | AS |
|---|---|---|
| **% Block at 50 mV and Endocardium** | 5±21 (4) | 19±18 (4) |
| **% Block at 50 mV and Epicardium** | 9±17 (6) | 20±17 (4) |

Values are expressed as mean±SD. Brackets indicate the number of cells. There was no significant difference between controls and AS data based on an unpaired *t* test.

Fig 15 **Methoxamine blocked $I_{to}$ more in control than in AS myocytes in both endocardium and epicardium.** Representative currents showing $I_{to}$ measured at +40mV at baseline (**1**) and in the presence of 100μM Methoxamine (**2**). (**A** and **B**) Currents from control endocardial and epicardial myocytes respectively. (**C** and **D**) Currents from AS endocardial and epicardial myocytes respectively. Please refer to Table 2. for mean values, statistics and n values.

Fig 15

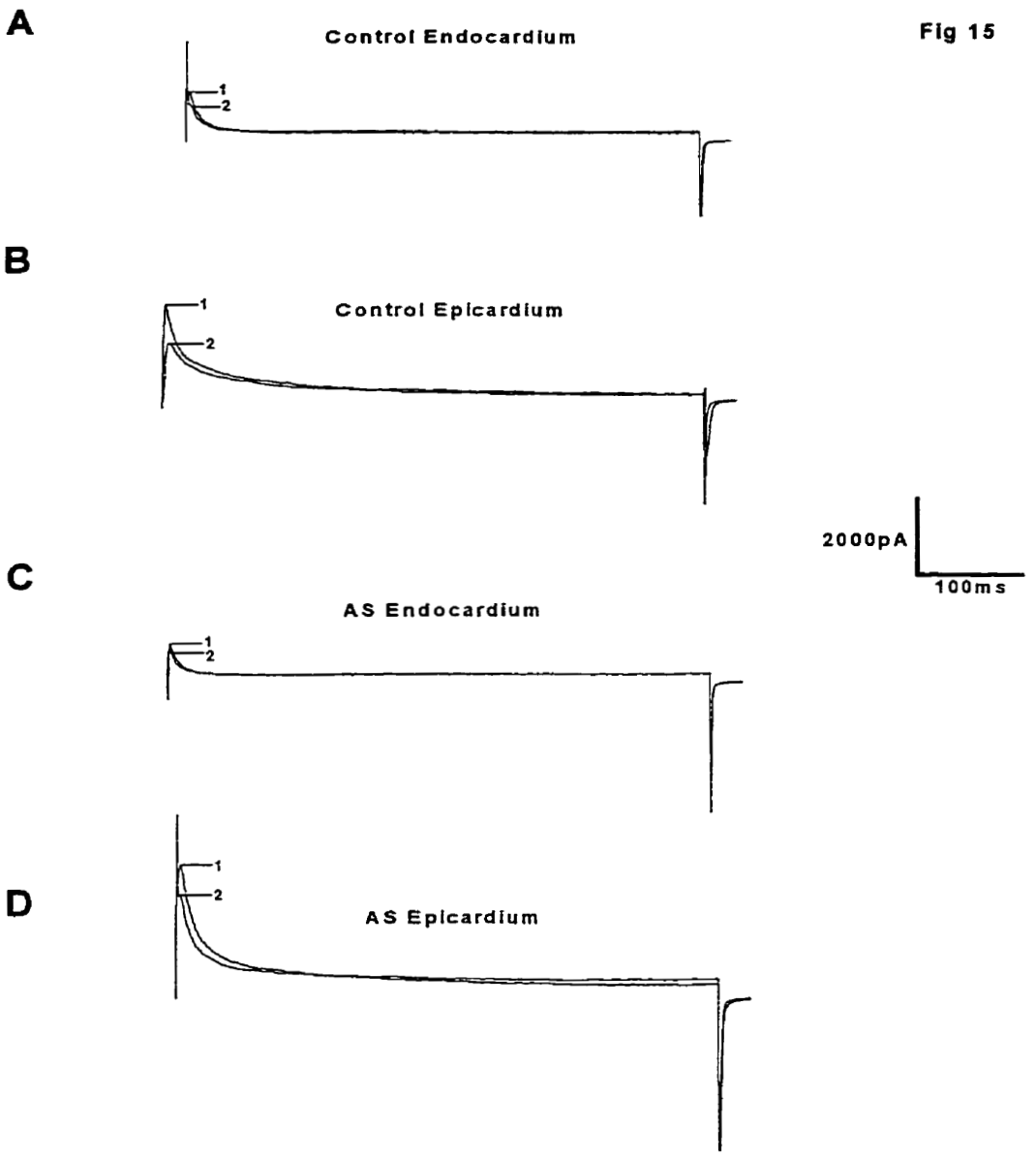
A
Control Endocardium
1
2
B
Control Epicardium
1
2
2000pA
100ms
C
AS Endocardium
1
2
D
AS Epicardium
1
2

Fig 16 **Methoxamine blocked $I_{K1}$ more at -110mV than at -60mV**. However, the amount of block was similar in control and AS as well as endocardium and epicardium. Representative currents showing $I_{K1}$ measured at -110 and -60mV at baseline (**1**) and in the presence of 100μM Methoxamine (**2**). (**A** and **B**) Currents from control endocardial and epicardial myocytes respectively. (**C** and **D**) Currents from AS endocardial and epicardial myocytes respectively. Please refer to Table 3. for mean values, statistics and n values.

Fig 16

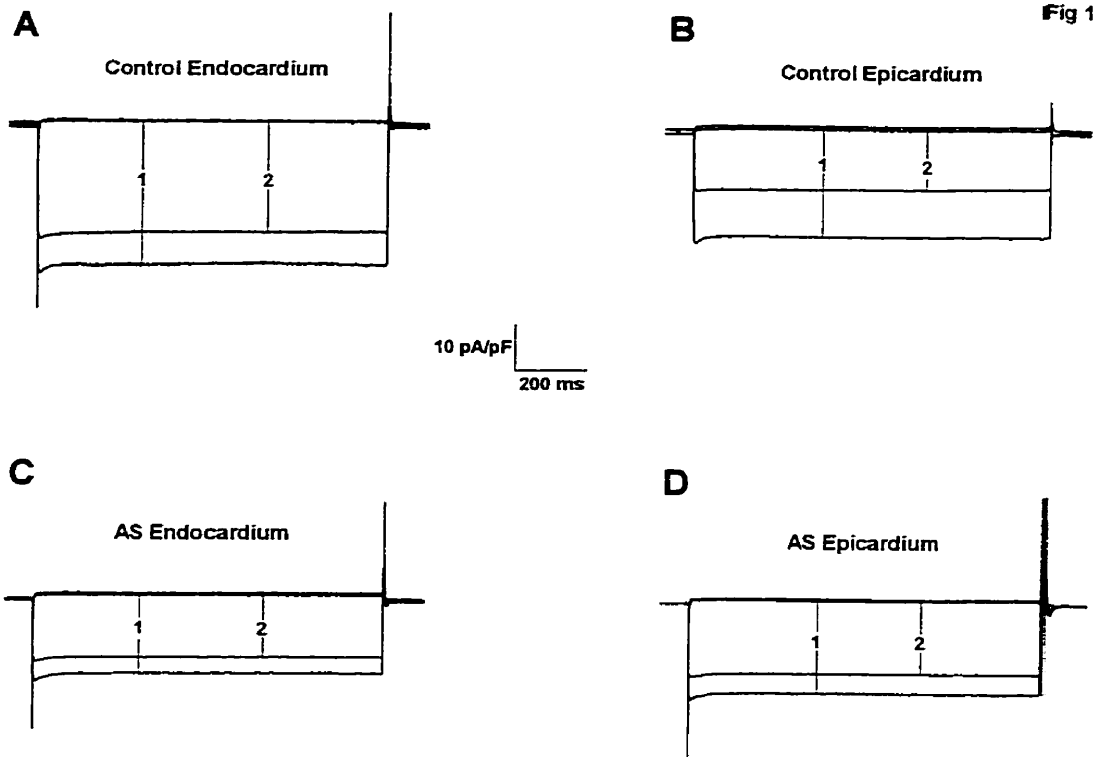
A
Control Endocardium
1
2
B
Control Epicardium
1
2
10 pA/pF
200 ms
C
AS Endocardium
1
2
D
AS Epicardium
1
2

Fig 17 **Methoxamine application had little effect on control $I_{Kr}$ tail currents.** However the amount of block was similar in endocardium and epicardium. Representative currents showing control $I_K$ tails at baseline and in the presence of 100μM Methoxamine. Shown are tail currents from endocardial (**A**) and epicardial (**B** myocytes respectively. Please refer to Table 4. for mean values, statistics and n values.

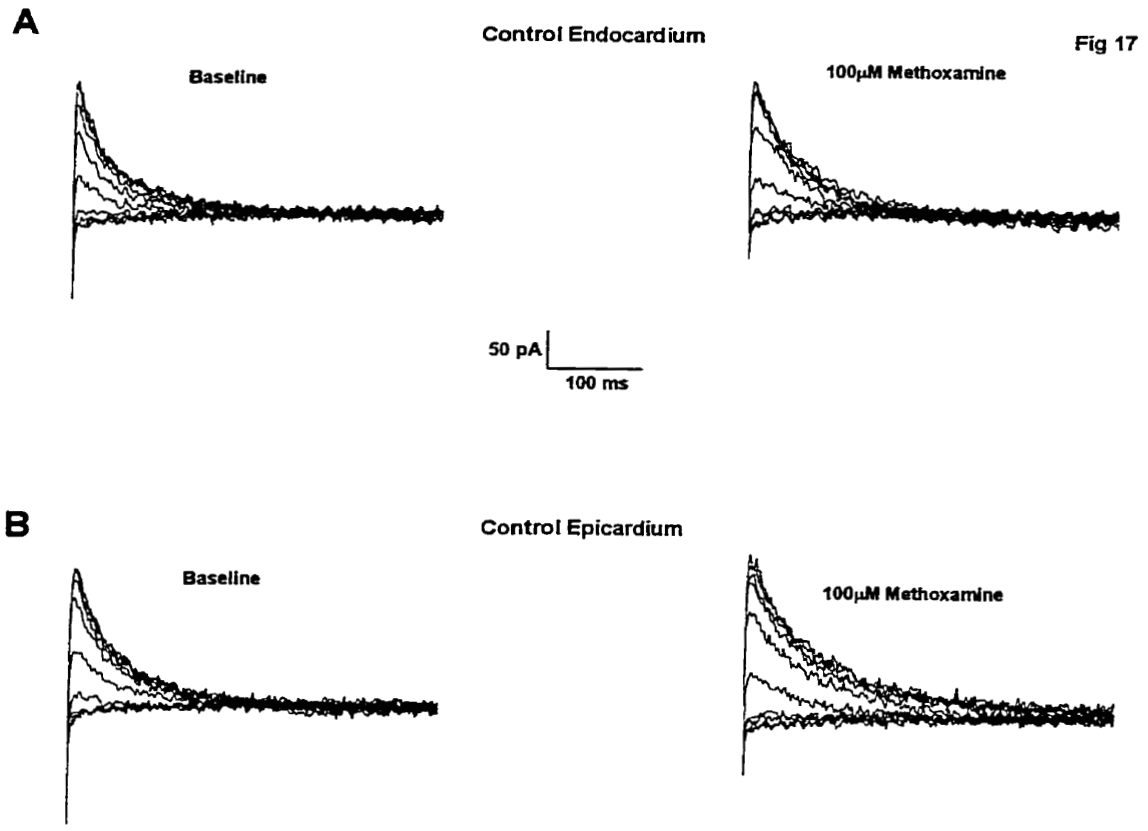
A
Control Endocardium
Baseline
100μM Methoxamine
50 pA
100 ms
B
Control Epicardium
Baseline
100μM Methoxamine

Fig 17

Fig 18 **Methoxamine application had little effect on AS $I_{Kr}$ tail currents**. However the amount of block was similar in endocardium and epicardium. Representative currents showing AS $I_K$ tails at baseline and in the presence of 100μM Methoxamine. Shown are tail currents from endocardial (**A**) and epicardial (**B**) myocytes respectively. Please refer to Table 4. for mean values, statistics and n values.

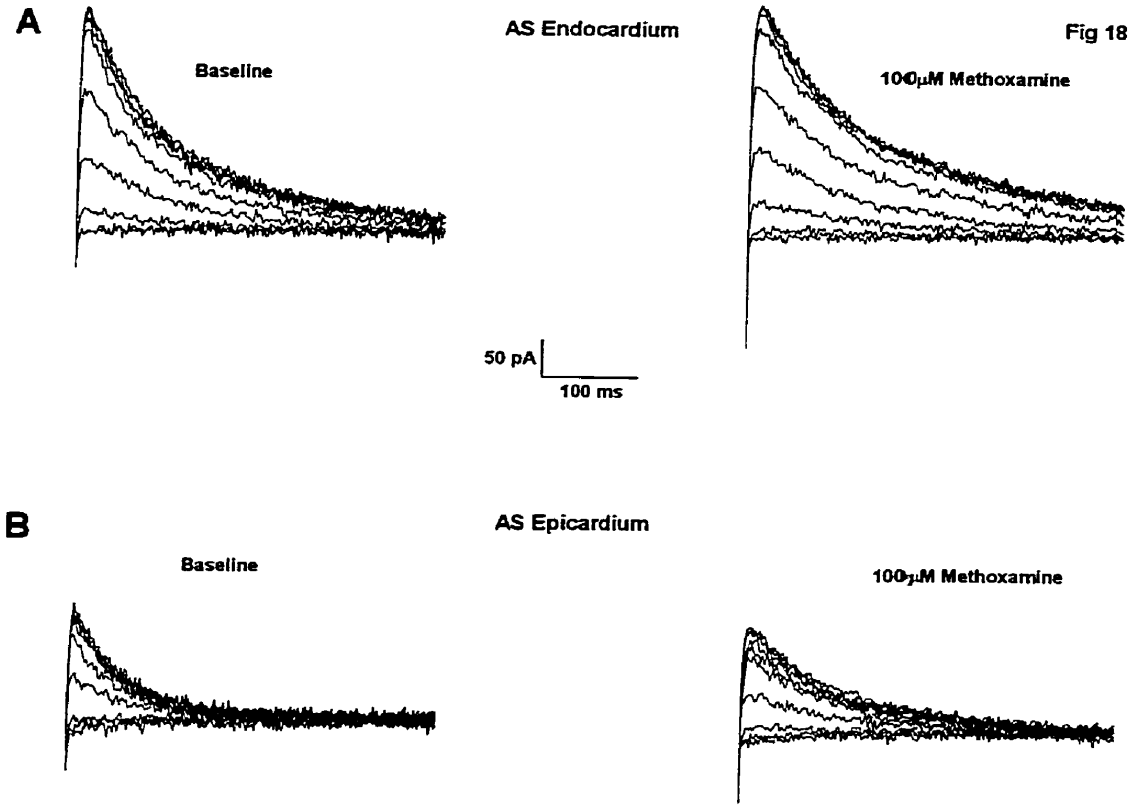
A
AS Endocardium
Fig 18
Baseline
100μM Methoxamine
50 pA
100 ms
B
AS Epicardium
Baseline
100μM Methoxamine

# Discussion : Chapter 5

Cardiac hypertrophy studied approximately 100 days after suprarenal banding of the aorta produced more pronounced reductions in $I_{to}$ in the epicardium than endocardium; reduction of $I_{K1}$ only in the endocardium and an exaggeration of the transmural spatial heterogeneity of $I_{Kr}$ density. In addition, response of $I_{to}$ to methoxamine was attenuated in myocytes from hypertrophied hearts whereas the response of $I_{K1}$ and $I_{Kr}$ to methoxamine was not. From these data we conclude that chronic in vivo $\alpha_1$-adrenergic stimulation likely contributes to the hypertrophy-induced reduction $I_{to}$ but not $I_{K1}$ .

For reference and review, this was the conceptual model that was being evaluated in this project to deduce the possible mechanistic interactions that occur in pressure overload induced LVH.

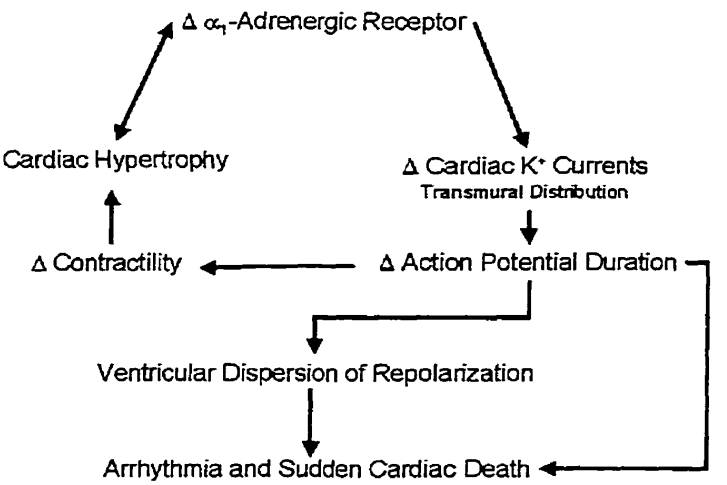

## 5.1 Indices of Hypertrophy

Based on the parallel significant increases seen in BP, cell capacitance, and heart wet weight/body weight ratio in hypertrophied rabbits compared to control, the model of left ventricular pressure overload successfully induced cardiac hypertrophy used in this project. This is in keeping with other papers that have used this model of LVH to evaluate other aspects of LVH.

## 5.2 Changes in the Depolarization Activated Outward $K^+$ Current

### SUMMARY

The depolarization-activated outward $K^+$ current was 4-AP sensitive. The current density of $I_{to}$ was decreased by LVH and that decrease was regionally dependent. Significant decreases were seen in control versus AS in both the endocardium and epicardium. Even though there were no differences in endocardium versus epicardium for either control or AS, the reduction in $I_{to}$ density was greater in the epicardium than in the endocardium. Similarly, $I_{sus}$ density was significantly decreased in control versus AS, but only in the epicardium. These observations suggest a regional heterogeneity of the effects of LVH on the depolarization-activated outward $K^+$ current.

## COMPARISON TO PREVIOUS STUDIES

The above observations are similar to the observations found by McIntosh *et al.*, 1998. However in their study, LVH decreased both epicardial and endocardial $I_{to}$ to a similar degree. In this study, we found that the LVH-induced decrease in $I_{to}$ was more pronounced in the epicardium than in the endocardium. A possible explanation for the discrepancy in results could be that McIntosh *et al.* used a different model of LVH. They developed LVH by inducing perinephritis in the rabbits. In addition, the age of rabbits used in their study was much younger and smaller (1.5 – 2kg compared to 2.5 to 3.0kg) than the rabbits used in this project. Moreover, McIntosh *et al.* studied rabbits 10 weeks after perinephritis-induced hypertension as opposed to this project that studied rabbits 100+days after banding. Also, one might argue that the observation in the manuscript of Fedida *et al.* 1991, that in normal rabbit hearts, epicardial $I_{to}$ was significantly greater than endocardial $I_{to}$ was not in keeping with the results found in this project. The explanation for this discrepancy was that Fedida *et al.* stated that the differences in $I_{to}$ between the epicardium and endocardium were only significant at voltages +40mV and higher (Fedida *et al.*, 1991). The results in this project showed a trend that epicardial $I_{to}$ was greater than endocardial $I_{to}$ in normal rabbits, but the voltages measured stopped after +40mV. If measurements had been made above +40mV, a significant difference in $I_{to}$ regional distribution might have been seen. However, the range of voltages tested in the present study were limited to those that are physiologically relevant.

## 5.3 Changes in the Inwardly Rectifying $K^+$ Current, $I_{K1}$

### SUMMARY

The inwardly rectifying $K^+$ current was barium sensitive. The current density of $I_{K1}$ was decreased by LVH and that decrease was regionally dependent. A significant decrease was seen in control versus AS in the endocardium only. There were no differences between endocardium and epicardium for either control or AS.

### COMPARISON TO PREVIOUS STUDIES

Since only endocardial $I_{K1}$ was affected by LVH, this suggested that endocardial $I_{K1}$ was more sensitive to the effects of LVH than epicardial $I_{K1}$. However, the decrease in $I_{K1}$ density was modest (though significant). In the study by McIntosh *et al.,* 1998, it was observed that $I_{K1}$ was decreased markedly and to a similar degree in both endocardium and epicardium. A possible explanation for the discrepancy in results could be that McIntosh *et al.* used a different model of LVH. Moreover, McIntosh *et al.* studied rabbits 10 weeks after perinephritis-induced hypertension as opposed to this project that studied rabbits 100+days after banding. It is important to note that in their study, only 5 hypertrophied endocardial cells were studied versus 7 controls. Also, only 4 hypertrophied epicardial cells were studied versus 7 controls (ie: they used a smaller sample size).

## 5.4 Changes in the Delayed Rectifying $K^+$ current, $I_K$

### SUMMARY

The delayed rectifying $K^+$ tail current was dofetilide-sensitive. This suggested that the tail current was predominantly $I_{Kr}$. The tail current density of $I_{Kr}$ showed regional heterogeneity between endocardium and epicardium and this heterogeneity was augmented by LVH. However, there were no significant differences between control and AS myocytes from either endocardium or epicardium. Even though there were no significant differences, there appeared to be a decreasing trend of AS $I_{Kr}$ versus control $I_{Kr}$ in the epicardium. This would explain the augmentation of $I_{Kr}$ regional heterogeneity seen in LVH. Furthermore, this observation added further support to the overall notion of this project that the epicardium is more sensitive to the modulatory effects of LVH on the repolarization $K^+$ currents.

### COMPARISON TO PREVIOUS STUDIES

No previous studies have reported the effects of LVH on $I_K$ tail currents in rabbit. Thus the $I_K$ data presented in this project was novel. In normal guinea pig (where $I_{Kr}$ tails have been measured), $I_{Kr}$ tail current density was found to be greater in the epicardium than in the endocardium (Bryant *et al.,* 1998). This was found to be the opposite in rabbits, which showed a greater $I_{Kr}$ tail current density in

endocardium than in epicardium. This discrepancy may be the result of species differences.

## 5.5 Effects of *in vitro* Administration of 100μM Methoxamine on $K^+$ Currents

### DEPOLARIZATION-ACTIVATED OUTWARD $K^+$ CURRENT

SUMMARY

It was found that the depolarization activated outward $K^+$ current was markedly suppressed by 100μM methoxamine. This was in keeping with previous results done by Braun *et al.*, 1990. However, the effect of acute *in vitro* methoxamine administration had not yet been previously reported in LVH conditions. What was novel in this project was that the inhibitory effects of methoxamine were attenuated in LVH myocytes versus control myocytes in both endocardium and epicardium. Thus, the effect of LVH on methoxamine suppression of the depolarization-activated outward $K^+$ current was regionally homogeneous.

SIGNIFICANCE OF THE RESULTS

The observation that the inhibitory effect of methoxamine on the depolarization-activated outward $K^+$ current is altered in LVH supports the notion that

the $\alpha_1$-adrenergic receptor contributes to the chronic regulation of the depolarization activated outward $K^+$ current in LVH.

## COMPARISON TO PREVIOUS STUDIES

Previous studies have reported that the $\alpha_1$-adrenergic receptor stimulation could contribute to the development of LVH. Also, $\alpha_1$-adrenergic agonists, like methoxamine have been shown to suppress $I_{to}$ acutely (Braun *et al.,* 1990). This suggests that chronic $\alpha_1$-adrenergic receptor stimulation may cause a chronic reduction in depolarization-activated outward $K^+$ current density in the development of LVH.

## EXPLANATION OF RESULTS

A possible explanation for the observed reduction in methoxamine's inhibitory effect on the depolarization outward $K^+$ current in LVH could be based on this correlation. Chronic $\alpha_1$-adrenergic stimulation in LVH would lead to chronic suppression of the depolarization-activated outward $K^+$ current. When methoxamine was added acutely, the majority of depolarization-activated outward $K^+$ channels would have been suppressed already, leaving a reduced number of active channels. Moreover, acute methoxamine would have only these remaining channels to suppress and thus it would seem that the effect of methoxamine might be expected to be less in LVH myocytes.

## INWARDLY RECTIFYING $K^+$ CURRENT

### SUMMARY AND COMPARISON TO PREVIOUS STUDIES

Acute methoxamine was also able to inhibit $I_{K1}$ current density in both the inward and outward portions of $I_{K1}$. Methoxamine inhibited the inward portion much greater than the outward portion of $I_{K1}$. However, there were no significant differences in the inhibitory effect in control versus AS and in endocardium versus epicardium. This is in keeping with the results published by Fedida *et al.,* 1991.

### SIGNIFICANCE OF THE RESULTS

The above observations would suggest that the $\alpha_1$-adrenergic receptor does not contribute to the LVH-induced modulation of $I_{K1}$. According to Fedida *et al.,* the inhibitory effect of acute methoxamine was independent of the protein kinase C (PKC) signal transduction pathway that is associated with the $\alpha_1$-adrenergic receptor. This observation further supports the notion that the modulation of $I_{K1}$ in LVH is not directly linked to the $\alpha_1$-adrenergic receptor.

## DELAYED RECTIFYING $K^+$ CURRENT

SUMMARY

Acute methoxamine was also able to inhibit $I_{Kr}$ tail current density. However, the inhibitory effect was marginal in AS versus control myocytes isolated from endocardium and epicardium. Also, the effect was similar in all subgroups examined.

## COMPARISON TO PREVIOUS STUDIES

Tohse *et al.,* found that $\alpha_1$-adrenergic stimulation enhanced $I_K$ in guinea pig through a PKC dependent pathway. This discrepancy could be explained due to species variability. Guinea pig $I_K$ has been shown to contain a large slow component of the delayed rectifier ($I_{Ks}$) and that the $I_K$ in guinea pig is a mix of $I_{Ks}$ and $I_{Kr}$. In rabbits, it has been previously reported that $I_{Ks}$ is either lacking or is very small in rabbit ventricular myocytes (Carmeliet *et al.,* 1992, Cordeiro *et al.,* 1998). Also, Tohse *et al.* did not examine tail currents, only the activated outward current of $I_K$.

## SIGNIFICANCE OF THE RESULTS

Since the inhibitory effect of methoxamine was similar in controls and AS, and in endocardium and epicardium, this would suggest that the $\alpha_1$-adrenergic receptor did not contribute to the LVH-induced augmentation of $I_{Kr}$ transmural distribution.

## 5.6 PROLONGATION OF APD

The overall results of this project showed that $I_{to}$ and $I_{sus}$ were modulated most by LVH. Thus, one could suggest that in this rabbit model, it would be $I_{to}$ and $I_{sus}$ that would predominantly contribute to a prolongation in APD due to LVH. This prolongation in APD could result in the formation of EADs that could lead to arrhythmia and even sudden cardiac death.

## 5.7 DISPERSION OF VENTRICULAR REPOLARIZATION

### NORMAL RABBITS

Previous studies have shown that there is an underlying dispersion of repolarization in normal rabbit hearts (Fedida *et al.*, 1988, Gillis *et al.*, 1998, Liu *et al.*, 1993) According to McIntosh *et al.*, 1998, in normal rabbits, APD measured from the endocardium was prolonged compared to APD measured from the epicardium. This is consistent with the underlining dispersion of repolarization seen in normal rabbits in my study. The baseline APD regional heterogeneity was explained by Fedida *et al.* who showed that there were regional differences in $I_{to}$ density in normal rabbits. In normal rabbits, it was observed that epicardial $I_{to}$ current density was larger than endocardial $I_{to}$. A larger $I_{to}$ would result in a shorter APD.

### HYPERTROPHIED RABBITS

In LVH, the dispersion of ventricular repolarization has been shown to be increased. In addition, LVH causes a "reversal" of the APD transmural distribution (McIntosh *et al.*, 1998, Shimizu *et al.*, 1999) These significant alterations in the dispersion of ventricular repolarization could lead to arrhythmia and sudden cardiac death. Based on the results from McIntosh *et al.* as well as the results obtained in this project, it is LVH-induced modulation of $I_{to}$ that results in the observed regionally heterogeneous prolongation of APD and subsequent alteration in the dispersion of ventricular repolarization in rabbit. However, the $I_{to}$ results of McIntosh *et al.* can

only partially account for their own observation that LVH caused a "reversal" of APD transmural distribution. If the LVH-induced decrease in $I_{to}$ were similar in endocardium and epicardium, a significant prolongation of APD in both endocardium and epicardium would occur. However, the endocardial APD would still be more prolonged than the epicardial APD by following the same trend in APD transmural distribution seen in normal rabbit hearts. Our observation that the epicardial APD was more prolonged than the endocardial APD suggested that the epicardium was more sensitive to the effects of LVH than the endocardium. The observation made in this project that the LVH-induced decrease in $I_{to}$ was more pronounced in the epicardium than in the endocardium would explain the "reversal" of APD transmural distribution observed by McIntosh *et al.* A more pronounced decrease in epicardial $I_{to}$ than endocardial $I_{to}$ would result in a longer APD in the epicardium than in the endocardium and thus lead to the "reversal" of APD transmural distribution.

## 5.8 Future Studies

Due to the complexity of the process involved in the development of left ventricular pressure overload-induced cardiac hypertrophy, further studies are needed to increase our understanding of this intriguing process. However, these studies are beyond the research for this Master's degree.

### MOLECULAR MECHANISMS OF LVH

One area of study would be the chronic regulation of these repolarization $K^+$ currents in LVH. For example, changes in protein biosynthesis would examine if there were alterations in the production of $K^+$ channel proteins in LVH as well as regional differences in endocardium and epicardium. Examining the changes in mRNA levels of MERG ($I_{Kr}$), IRK ($I_{K1}$) and Kv4.2 and Kv4.3 ($I_{to}$) in both control and AS rabbits (in both endocardium and epicardium) would indirectly assess the kinetics of protein biosynthesis of these repolarization $K^+$ currents in LVH. The development of antibodies to the protein products of MERG, IRK and Kv4.2 and Kv4.3 would be another useful tool for the study of protein biosynthesis in LVH. These antibodies could be used as specific protein probes to examine individual sarcolemmal $K^+$ channel protein levels, which could be correlated with any changes in mRNA levels of that particular gene product. Using both these tools, one would be able to examine the changes in kinetics of protein synthesis in LVH as well as regional distribution of these repolarization $K^+$ channels.

## $\alpha_1$-ADRENERGIC REGULATORY MECHANISMS IN LVH

To further elucidate the mechanisms involved with $\alpha_1$-adrenergic regulation of the depolarization activated outward $K^+$ current in LVH, chronic treatment (*in vivo*) of AS rabbits with pertussis toxin could yield interesting results on the involvement of G proteins in $K^+$ current regulation. In addition, there are many isoforms of PKC. It has been shown that the distributions of these isoforms within a cardiac myocyte are altered in LVH (Puceat *et al.,* 1996). In light of this observation, various isoforms of PKC may have different functional roles in the development of LVH. It is possible that one or more PKC isoforms are specifically activated to regulate repolarization $K^+$ currents responsible for repolarizing the cardiac APD. Further studies should be done to determine the functional roles of these various isoforms of PKC and their involvement with LVH.

## 5.9 Limitations

1. On the day of the study, most of the rabbits on both groups were old and large (4-5kg). In the literature it has been shown that age does affect cardiac function and its underlining electrophysiology. Also, the yield of high quality cells needed for voltage clamp experiments diminishes with age. The results of this study might be different if younger animals were used. However, the age factor could not have been avoided due to the long wait needed for LVH to develop in this model.

2. Since all whole-cell voltage clamp experiments were done at 37°C, the kinetics of the depolarization-activated outward $K^+$ currents were extremely fast. The result in some cases was that the peak outward current was embedded into the capacitive transient. Compensation for capacitance and series resistance (to reduce the amount of capacitive transient) was performed on all experiments, however only partial compensation (approx. 40%) was obtained due to the large size of the myocytes used in the experiments. This was unavoidable due to limitations in the voltage clamp hardware.

3. $I_K$ tail currents were only examined in this study because they were significantly blocked by dofetilide suggesting that the tail current was predominantly $I_{Kr}$. $I_{Ks}$ was not studied due to evidence in the literature that $I_{Ks}$ in rabbit was very small to nonexistent (Cordeiro *et al.,* 1998, McIntosh *et al.,* 1998). However, for future studies, $I_{Ks}$ should be examined (maybe in different species like guinea pig) and

may provide further understanding of the effects of LVH and regional dispersion on $I_K$.

4. The depolarization-activated outward $K^+$ current was only measured up to +40mV. However, in light of the literature of the regional distribution of $I_{to}$ in heart, it was seen that pulses past +40mV were needed to observe significant changes in $I_{to}$ distribution in heart. Since voltage clamp measurements were done at 37°C, pulses above +40mV were not feasible due to the extremely fast inactivation of the peak outward current. At pulses +50mV and higher, the peak outward current was superimposed onto the transient capacitance and thus making accurate measurements of the peak outward current at those pulses impossible.

5. In the acute methoxamine experiments, only one dose was used to examine the effects of methoxamine on the repolarization $K^+$ currents. This dose was chosen based on previous literature that performed dose-response relationships with methoxamine on the currents studied. Similar dose-response relationships could not be obtained in this project due to the size and age of the myocytes obtained. The myocytes were all from old rabbits with significant cardiac disease in some cases. The resulting myocytes were very fragile and did not last long enough for a thorough dose response experiment. Therefore, only one dose was chosen from the literature in order to produce a maximal physiological effect.

## Conclusion : Chapter 6

By following the model set forth at the beginning of this project, it was determined that LVH altered cardiac repolarization $K^+$ currents by modulating their current densities ($I_{to}$, $I_{sus}$, and $I_{K1}$) and augmented their transmural regional heterogeneities ($I_{to}$, $I_{sus}$, and $I_{Kr}$). The $\alpha_1$-adrenergic receptor was found to have an involvement in the chronic modulation of the depolarization-activated outward $K^+$ current in rabbit LVH. It was this chronic modulation of the depolarization-activated outward $K^+$ current that could contribute to the prolongation of APD and the alterations in the dispersion of ventricular repolarization often seen in rabbit LVH. These alterations in cardiac electrophysiology would contribute to the abnormal cardiac rhythms seen in LVH that could lead to arrhythmia and sudden cardiac death.

# References


1. Antzelevitch C, Shimizu W, Yan GX, Sicouri S. Cellular basis for QT dispersion. *J. Electrocardiol.* 1998:30 Suppl;168-175

2. Bogoyevitch MA, Andersson MB, Gillespie-Brown J, Clerk A, Glennon PE, Fuller SJ, Sugden PH. Adrenergic receptor stimulation of the mitogen-activated protein kinase cascade and cardiac hypertrophy. *Biochem. J.* 1996:314;115-121

3. Braun AP, Fedida D, Giles WR. Activation $\alpha_1$-adrenoceptors modulates the inwardly rectifying potassium currents of mammalian atrial myocytes. *Pflugers Arch.* 1992:421;431-439

4. Braun AP, Fedida D, Clark RB, Giles WR. Intracellular mechanisms for $\alpha_1$-adrenergic regulation of the transient outward current in rabbit atrial myocytes. *J. Physiol.* 1990:431;689-712

5. Bril A, Forest MC, Gout B. Ischemia and reperfusion-induced arrhythmias in rabbits with chronic heart failure. *Am. J. Physiol.* 1991:261(30);H301-H307

6. Bryant SM, Wan X, Shipsey SJ, Hart G. Regional differences in the delayed rectifier current ($I_{Kr}$ and $I_{Ks}$) contribute to the differences in action potential

duration in basal left ventricular myocytes in guinea pig. *Cardiovasc Res.* 1998:40(2); 322-331

7. Calderone A, Takahashi N, Izzo NJ Jr., Thaik CM, Colucci WS., Pressure and volume-induced left ventricular hypertrophies are associated with distinct myocyte phenotypes and differential induction of peptide growth factor mRNAs. *Circulation.* 1995:92(9); 2385-2390

8. Carmeliet E., Voltage and time-dependent block of the delayed $K^+$ current in cardiac myocytes by dofetilide. *J Pharmacol Exp Ther* 1992:262;809-817.

9. Casis O, Iriate M, Gallego M, Sanchez-Chapula A. Differences in regional distribution of $K^+$ current densities in rat ventricle. *Life Sc.* 1998:63(5);391-400

10. Cordeiro JM, Spitzer KW, Giles WR. Repolarizing $K^+$ currents in rabbit heart Purkinje cells. *J. Physiol.* 1998:508(3);811-823

11. Corr PB, Heathers GP, Yamada KA. Mechanisms contributing to the arrhythmogenic influences of alpha$_1$-adrenergic stimulation in the heart. *Am. J. Med.* 1989:87(Suppl 2A);19S-25S

12. Corr PB, Shayman JA, Kramer JB, Kipnis RJ. Increased alpha-adrenergic receptors in ischemic cat myocardium. *J. Clin. Invest.* 1981:67;1232-1236

13. Crick SJ, Anderson RH, Ho SY, Sheppard MN. Localization and quantitation of autonomic innervation in porcine heart II: endocardium, myocardium and epicardium. *J. Anat.* 1999:195;359-373

14. DiFrancesco D, Ferroni A, Visentin S. Barium-induced blockade of the inward rectifier in calf Purkinje fibres. *Pflugers Arch.* 1984:402(4)446-453

15. Dillon JS, Gu XH, Nayler WG. Alpha$_1$-adrenoceptors in the ischemic and reperfused myocardium. *J. Mol. Cell. Cardiol.* 1988:20;725-735E

16. Endoh M, Blinks JR. Actions of sympathomimetic amines on the $Ca^{2+}$ transients and contractions of rabbit myocardium: reciprocal changes in myofibrillar responsiveness to $Ca^{2+}$ mediated through alpha and beta adrenoceptors. *Circ. Res.* 1988:62;247-265

17. Fedida D, Braun AP, Giles WR. $\alpha_1$-adrenoceptors reduce background $K^+$ current in rabbit ventricular myocytes. *J. Physiol.* 1991:441;673-684

18. Fedida D, Braun AP, Giles WR. $\alpha_1$-adrenoceptors in myocardium: functional aspects and transmembrane signaling mechanisms. *Physiol. Rev.* 1993:73(2);469-487

19. Fedida D, Giles WR. Regional variations in action potentials and transient outward current in myocytes isolated from rabbit left ventricle. *J. Physiol.* 1991:442;191-200

20. Giles WR, Imaizumi Y. Comparison of Potassium currents in rabbit atrial and ventricular cells. *J. Physiol.* 1988:405;123-145

21. Giles WR, van Ginneken A. A transient outward current in isolated cells from the crista terminalis of rabbit heart. *J. Physiol.* 1985:368;243-264

22. Gillis AM, Geonzon RA, Mathison HJ, Kulisz E, Lester WM. The effects of barium, dofetilide and 4-aminopyridine (4-AP) on ventricular repolarization in normal and hypertrophied rabbit heart. *J. Pharm. Exp. Therapeut.* 1998:285(1);262-285

23. Gillis AM, Mathison HJ, Kulisz E, Lester WM. Dispersion of ventricular repolarization in left ventricular hypertrophy: Influence of afterload and dofetilide. *J. Cardiovasc. Electrophysiol.* 1998:9(9);988-997

24. Guo W, Kamiya K, Yasui K, Kodama I, Toyama J. Alpha$_1$-adrenoceptor agonists and IGF-1, myocardial hypertrophic factors, regulate the Kv1.5 $K^+$ channel expression differentially in cultured rat ventricular cells. *Pflugers Arch.-Eur. J. Physiol.* 1998:436;26-32

25. Guyton AC. Textbook of Medical Physiology 8th Edition. WB Saunders Company. 1991

26. Hayashi S, Umemura S, Ashino K, Hirawa N, Toya Y, Abe Y, Ishii M. $\alpha_1$-adrenergic receptors in cardiac ventricles of Dahl rats. *Am. J. Hypertens.* 1995:8;850-854

27. Hescheler J, Nawrath H, Tang M, Trautwein W. Adrenoceptor-mediated changes of excitation and contraction in ventricular heart muscle from guinea pigs and rabbits. *J. Physiol (Lond)* 1988:397;657-670

28. Hille B. Ionic Channels of Excitable Membranes. Sinauer Associates. Sunderlan, MA 1992.

29. Imai C, Tozawa M, Sunagawa O, Muratani H, Takishita S, Fukiyama K. Alterations of alpha1-adrenergic receptor densities in right and left ventricles of spontaneously hypertensive rats. *Biol. Pharm. Bull.* 1995:18(7);1001-1005

30. LaMorte VJ, Thorburn J, Absher D, Spiegel A, Brown JH, Chien KR, Feramisco JR, Knowlton KU. $G_q$ and ras dependent pathways mediate hypertrophy of neonatal rat ventricular myocytes following alpha$_1$-adrenergic stimulation. *J. Biol. Chem.* 1994:269(18);13490-13496

31. Li K, He H, Li C, Sirois P, Rouleau JL. Myocardial alpha1-adrenoceptor: intropic effect and physiologic and pathologic implications. *Life Sci.* 1997:60(16);1305-1318

32. Liu DW, Gintant GA, Antzelevitch C. Ionic basis for electrophysiological distinctions among epicardial, midmyocardial, and endocardial myocytes from the free wall of the canine left ventricle. *Circ. Res.* 1993:72(3);671-687

33. McIntosh MA, Cobbe SM, Kane KA, Rankin AC. Action potential prolongation and potassium currents in left ventricular myocytes isolated from hypertrophied rabbit hearts. *J. Mol. Cell. Cardiol.* 1998:30;43-53

34. Meszaros J, Ryder K, Hart G. transient outward current in catecholamine-induced cardiac hypertrophy in the rat. *Am. J. Physiol.* 1996:271(40);H2360-H2367

35. Milano CA, Dolber PC, Rockman HA, Bond RA, Venable ME, Allen LF, Lefkowitz RJ. Myocardial expression of a constitutively active alpha 1B-adrenergic receptor in transgenic mice induces cardiac hypertrophy. *Proc. Natl. Acad. Sci.* 1994:91(21);10109-10113

36. Milnor WR. Cardiovascular Physiology. Oxford University Press. 1990;22-25, 83-86

37. Nabauer M, Kaab S. Potassium channel down-regulation in heart failure. *Cardiovasc. Res.* 1998:37;324-334

38. Potreau D, Gomez JP, Fares N. Depressed transient outward current in single hypertrophied cardiomyocytes isolated from the right ventricle of ferret heart. *Cardiovasc Res.* 1995:30;440-448

39. Puceat M, Vassort G. Signalling by protein kinase C isoforms in the heart. *Mol. Cell. Biochem.* 1996:157;65-72

40. Randhawa A, Singal PK. Pressure overload-induced cardiac hypertrophy with and without dilation. *J. Am. College Cardiol.* 1992:20(7);1569-1575

41. Rohrer DK, Kobilka BK. G-protein-coupled receptors: Functional and Mechanistic Insights Through Altered Gene Expression. *Physiol. Rev.* 1998:78(1);35-52

42. Rokosh DG, Stewart AF, Chang KC, Bailey BA, Karliner JS, Camacho SA, Long CS, Simpson PC. Alpha1-adrenergic receptor subtype mRNAs are differentially regulated by alpha1-adrenergic and other hypertrophic stimuli in cardiac myocytes in culture and in vivo. Repression of alpha1B and alpha1D but induction of alpha1C. *J. Biol. Chem.* 1996:271(10);5839-5843

43. Sakmann B, Trube G. Conductance properties of single inwardly rectifying potassium channels in ventricular cells from guinea-pig heart. *J. Physiol.* 1984:347;641-657

44. Schunkert H, Weinberg EO, Bruckschlegel G, Riegger G, Lorell B. Alteration of growth responses in established cardiac pressure overload hypertrophy in rats with aortic banding. *J. Clin. Invest.* 1995:96;2768-2774

45. Shimizu W, Antzelevitch C. Cellular and ionic basis for T-wave alternans under long-QT conditions. *Circ.* 1999:99(11);1499-1507\

46. Shipsey SJ, Bryant SM, Hart G. Effects of hypertrophy on regional action potential characteristics in the rat left ventricle: a cellular basis for T-wave inversion? *Circ.* 1997:96(6);2061-2068

47. Siegelbuam SA, Tsien RW. Calcium-activated transient outward current in calf Purkinje fibres. *J. Physiol.* 1980:299;485-506

48. Simpson PC, Kariya K, Karns LR, Long CS, Karliner JS. Adrenergic hormones and control of cardiac myocyte growth. *Mol. Cell. Biochem.* 1991:104;35-43

49. Slavikova J, Goldstein M, Dahlstorm A. The postnatal development of tyrosine hydroxylase immunoreactive nerves in rat atrium, studied with

immunofluorescence and confocal laser scanning microscopy. *J. Auron. Nerv. Syst.* 1993:43;159-170

50. Tamai J, Hori M, Kagiya T, Iwakura K, Iwai K, Kitabatake A, Watanabe Y, Toshida H, Inoue M, Kamada T. Role of $\alpha_1$-adrenoceptor activity in progression of cardiac hypertrophy in guinea pig hearts with pressure overload. *Cardiovasc. Res.* 1989:23;315-322

51. Tohse N, Nakaya H, Kanno M. $\alpha_1$-adrenoceptor stimulation enhances the delayed rectifier $K^+$ current of guinea pig ventricular cells through the activation of protein kinase C. *Circ. Res.* 1992:71;1441-1446

52. Tomita F, Bassett AL, Myerburg RJ, Kimura S. Diminished transient outward currents in rat hypertrophied ventricular myocytes. *Circ. Res.* 1994:75(2);296-303

53. Wang Li. Potassium currents in mouse heart. PhD Dissertation. University of Calgary Department of Cardiovascular/Respiratory Sciences, Feb.1996

54. Wilber DJ, Lynch JL, Montgomery DG. Alpha-adrenergic influences in canine ischemic sudden death. Effects of alpha$_1$-adrenoceptor blockade with prazosin. *J. Cardiovasc. Pharmacol.* 1987:10;96-106